

## Wind Generator Co-Simulation with Fault Case Analysis

*Master of Science Thesis*

PETER MAKOLO

Department of Energy and Environment  
Division of Electric Power Engineering  
CHALMERS UNIVERSITY OF TECHNOLOGY  
Göteborg, Sweden 2013



# Wind Generator Co-Simulation with Fault Case Analysis

PETER MAKOLO

Department of Energy and Environment  
Division of Electric Power Engineering  
CHALMERS UNIVERSITY OF TECHNOLOGY  
Göteborg, Sweden 2013

Wind Generator Co-Simulation with Fault Case Analysis  
PETER MAKOLO

© PETER MAKOLO, 2013.

Department of Energy and Environment  
Division of Electric Power Engineering  
Chalmers University of Technology  
SE-412 96 Göteborg  
Sweden  
Telephone +46 (0)31-772 1000

Cover:

Above: The Co-Simulation circuit set-up

Below: Simulink representing control system, Maxwell model of a generator and a complete assembled generator together with control system

Chalmers Bibliotek, Reproservice  
Göteborg, Sweden 2013

## Abstract

As machine designs are becoming more complex and sophisticated, the process of verifying these designs and hence developing control strategies are therefore becoming more complicated, expensive and time consuming. In order to better understand the physics in complex machine designs, first-order harmonic models within dynamic simulations are becoming insufficient. However, co-simulation is now a proven way to handle and understand the physics of these complex machine designs. In this project, a finite-element-method model of a permanent magnet synchronous generator is developed. The generator model is then embedded/coupled with a PI control system model which is developed in Simulink. The process of coupling is facilitated with the use of Simplorer which links these two models. The complete embedded/coupled model is then simulated for a conventional torque control strategy of the generator. A fault case is introduced in the simulation in order to understand control strategies for the machine. Finally, simulation results indicate that it is possible to co-simulate a PMSM using Maxwell embedded in Simulink control system using Simplorer.

**Index Terms:** Simulink PI controller, Finite-Element-Method (FEM) of PMSM, Co-Simulation using Maxwell, Simplorer and Simulink.



## **Acknowledgements**

The outcome of this project was a result of untiring guidance and assistance from many people. I am extremely fortunate to have got this all along my project work. Whatever I have achieved is due to such guidance and assistance and therefore it is right and just to appreciate their contribution.

I would like to express my gratitude to my academic supervisor Joachim Härsjö for his tireless reading of my work and providing very constructive feedbacks. I am also thankful and fortunate enough to get constant encouragement, support and guidance from my examiner, Ola Carlson and all staff members of Chalmers University of Technology in Göteborg, Sweden especially the department of Energy and Environment and specifically Electric Power Engineering division. I had a wonderful studying environment at Chalmers which is the key to my academic achievement.

I heartily thank the Swedish Institute for Future Global Leaders for facilitating my studies in Sweden with a good scholarship which made my life very enjoyable for the two years of my stay in Sweden.

Last but not least, I would like to thank my lovely wife Lilian, my son Perlian Bunga, and my daughter Bless Wille for allowing me time and resources to invest in the study. Without their love, constant support, patience and prayers, I would not have managed to spend these two years of separation from them.

**To God be the Glory**

Peter Makolo  
Göteborg, Sweden, 2013





# Contents

<b>Abstract</b>	<b>iii</b>
<b>Acknowledgements</b>	<b>v</b>
<b>Contents</b>	<b>vii</b>
<b>Commonly used acronyms</b>	<b>ix</b>
<b>1 Introduction</b>	<b>1</b>
1.1 Project background . . . . .	1
1.2 Project objective . . . . .	1
1.3 Specific objectives/tasks . . . . .	2
1.3.1 Building a control system in Simulink . . . . .	2
1.3.2 Verification of the control system performance . . . . .	2
1.3.3 Building an FEM model of a permanent magnet generator . . . . .	2
1.3.4 Verification of the FEM model performance . . . . .	2
1.3.5 Embedding the FEM model in Simulink using Simplorer . . . . .	2
1.3.6 Simulating a conventional torque control strategy . . . . .	3
1.3.7 Evaluating a fault case . . . . .	3
1.4 Scope . . . . .	3
<b>2 Literature Review/Theory</b>	<b>5</b>
2.1 PMSG in wind power applications . . . . .	5
2.2 Dynamic model of PMSM in Simulink . . . . .	5
2.2.1 Modeling electrical part of PMSM . . . . .	6
2.2.2 Modeling PMSM in $\alpha\beta$ -system . . . . .	6
2.2.3 Modeling mechanical part of the PMSM . . . . .	8
2.2.4 Current controller design . . . . .	10
2.2.5 Speed controller design . . . . .	13
2.3 Simplorer . . . . .	14
2.3.1 Steps of coupling Simulink to Simplorer . . . . .	15
2.4 Maxwell . . . . .	15
2.4.1 How to build a generator in Maxwell . . . . .	16
2.4.2 Steps of coupling Maxwell to Simplorer . . . . .	16

<b>3</b>	<b>Modeling</b>	<b>17</b>
3.1	Model of the control system in Simulink . . . . .	17
3.1.1	General machine control arrangement . . . . .	17
3.1.2	S-Function of the machine . . . . .	17
3.1.3	Current control . . . . .	18
3.1.4	Current limiter . . . . .	19
3.1.5	Speed control . . . . .	19
3.1.6	Complete model of the control system . . . . .	20
3.2	Coupling of control system with Simplorer and verification . . . . .	20
3.3	Finite Element Method model of the PMSG . . . . .	22
3.4	Coupling of FEM model with Simplorer and verification . . . . .	27
3.5	Embedding FEM model to Simulink control system using Simplorer .	28
<b>4</b>	<b>Simulation</b>	<b>29</b>
4.1	Simulation approach . . . . .	29
4.2	Simulation of PMSM and controller in Simulink . . . . .	29
4.3	Co-simulation of PMSM in Simplorer and controller in Simulink . . .	32
4.4	Co-simulation of FEM model and Simplorer . . . . .	35
4.5	Co-Simulations of embedded FEM model in Simulink control system using Simplorer . . . . .	38
<b>5</b>	<b>Analysis, conclusion, recommendation and future work</b>	<b>43</b>
5.1	Analysis of simulation results . . . . .	43
5.1.1	Analysis and verification of the controller performance . . . .	43
5.1.2	Analysis and verification of co-simulation between Simulink and Simplorer . . . . .	43
5.1.3	Analysis and verification of FEM model performance . . . . .	44
5.1.4	Analysis of embedded FEM model in Simulink controller . . . .	44
5.1.5	Comparison of simulation results . . . . .	45
5.2	Conclusion . . . . .	46
5.3	Recommendation . . . . .	47
5.4	Future work . . . . .	48
	<b>References</b>	<b>49</b>
	<b>A ASPMSM Design Data</b>	<b>51</b>
	<b>B RMxpert Design graphs</b>	<b>59</b>

# Commonly used acronyms

AC - Alternating Current

ASPMSM - Adjustable-Speed Permanent Magnet Synchronous Machine

DC - Direct Current

DSPs - Digital Signal Processors

FEA - Finite Element Analysis

FEM - Finite Element Method

IGBT - Insulated-Gate Bipolar Transistor

IMC - Internal Model Control

MDL - Simulink model imported to Simplorer

PI - Proportional and Integral

PM - Permanent Magnet

PMSM - Permanent Magnet Synchronous Machine

PMSG - Permanent Magnet Synchronous Generator

$T_e$  - Electrodynamical Torque

$T_L$  - Load Torque

Ref. - Reference

2D - Two Dimension

3D - Three Dimension

RMxpert - Rotational Machine Expert

SiM2SiM - Simplorer to Simulink

FEA1.IT1 - Current phase1 of the Finite Element Analysis of the Maxwell model

FEA1.IT2 - Current phase2 of the Finite Element Analysis of the Maxwell model

FEA1.IT3 - Current phase3 of the Finite Element Analysis of the Maxwell model

FEA1.PHI - Position of the finite Element Analysis of the Maxwell model



# Chapter 1

## Introduction

### 1.1 Project background

Nowadays, the designs of machines are becoming more complex. As a result, the process of verifying these designs and developing control strategies are therefore becoming more complicated, expensive and time consuming [1]. Controls of complex machines have to get more and more sophisticated as well. New features and functions have to be constantly added to the main machine controls in order to differentiate the drives on the market. Complex controls are equipped with a variety of system parameters and incorporate extensive control algorithms of which are implemented in DSPs. With this high degree of complexity and the wide variety of domains involved in this kind of designs, there is a high demand for simulation and analysis tools [2].

However, in order to better understand the physics in a complex machine design, first-order harmonic models within dynamic simulations are becoming insufficient. A Finite Element Method (FEM) model embedded within a dynamic simulation seems to suite better the needs of complex control strategies, especially when the control actions to fault cases are taken into consideration. In short, it is said that, co-simulation is now a proven way to handle and understand the physics of these complex machine designs and hence facilitate the development of control strategies of complex machines [1].

### 1.2 Project objective

Being aware of the project background discussed above, this brings us to the main objective of this project which is to co-simulate a permanent magnet synchronous generator in order to develop control strategies of the machine. The co-simulation will mainly deal with a torque-controlled generator for wind power applications. The project will be facilitated with a combination of a FEM software, for this project is Ansoft Maxwell and dynamic simulation softwares, for this project are Simulink and Simplorer.

## 1.3 Specific objectives/tasks

In order to make the project easy to manage and handle, the main objective pointed out is further subdivided into various subtasks as:

- Building a control system in Simulink
- Verification of the control system performance
- Building a Finite Element model of the permanent magnet generator for wind power applications using Ansoft Maxwell software
- Verification of the FEM model performance
- Embedding the FEM model in Simulink with the use of Simplorer software (Linking all three software)
- Simulating a conventional torque control strategy for the generator
- Evaluation of some fault cases

### 1.3.1 Building a control system in Simulink

A PI control system is built in Simulink. The control system comprises an inner PI current control cascaded with an outer PI speed control all integrated together. This controller is then coupled to the generator for torque control.

### 1.3.2 Verification of the control system performance

Some simulations are done to verify the performance of the control system.

### 1.3.3 Building an FEM model of a permanent magnet generator

Ansoft Maxwell software is used to build the intended permanent magnet generator model for wind power application. The model built, would give the details of the generator analysis.

### 1.3.4 Verification of the FEM model performance

The FEM model of the generator is then coupled to Simplorer and some simulation are performed to verify the operation and performance of the model when connected to Simplorer. A line to line fault is also introduced in the simulation to observe how the machine responds to faults.

### 1.3.5 Embedding the FEM model in Simulink using Simplorer

The FEM model of the generator that has been built using Ansoft Maxwell, is then imported to Simplorer ready for coupling to the Simulink control system. The control system model that is built in Simulink is then added to Simplorer. Using the SiM2SiM interface link generated in Simulink by a special S-Function known as AnsoftSFunction, information from the FEM model can then be connected to the Simulink control system ready for co-simulation.

### **1.3.6 Simulating a conventional torque control strategy**

Having linked Simulink and FEM models in Simplorer, simulation is started in Simplorer. Simplorer calls the Simulink control system model and FEM model. When Simplorer starts the simulation, FEM model passes information to Simulink control system via AnsoftSFunction block. Simulink control system model further generates reference voltage to the machine. The reference voltage signals are passed through the AnsoftSFunction block to Simplorer and finally to the FEM model in Maxwell.

### **1.3.7 Evaluating a fault case**

A fault is introduced in the simulations to observe the behaviour of the controller.

## **1.4 Scope**

In reality, the system needs to have a converter between the controller and the machine. In the converter, one of the faults could also be introduced by short circuiting IGBTs to observe how the controller would react to such fault in the system. This project does not consider the converter, instead the voltages from the controller go direct to the machine.





# Chapter 2

## Literature Review/Theory

### 2.1 PMSG in wind power applications

In recent years, there has been an increasing interest of using renewable energy sources such as wind, solar, waves and others in electrical power production. There are many reasons for this interest. Shortage or limitation of availability of traditional energy sources in the near future, environmental problems, high prices for fuels and political reasons are some of the reasons [3] [4].

Looking at the wind power renewable energy source, the configuration of the system comprises of the large sized blades which make the rotating speed of the wind turbine to be slow. The wind turbine is usually coupled with the generator through a speed-up gearbox to reduce the overall size of the generator. However, the gearbox brings weight, generates noise, needs regular maintenance and increases losses [5]. The development of permanent magnet materials and decreasing costs of power electronics have made it possible to design a cost-effective wind power generation system with a direct driven permanent magnet (PM) generator which do not use a gearbox. The efficiency and reliability of the system can be improved compared with the conventional wind power generation system [5].

### 2.2 Dynamic model of PMSM in Simulink

Simulink being one of the known dynamic simulation software, is used to model the control system in this project. The theory explained in this part will be used to model the control system of the generator in question. Most of the theory in this part is mainly based on [6].

Fig. 2.1 shows the general configuration of the control system of the PMSM.

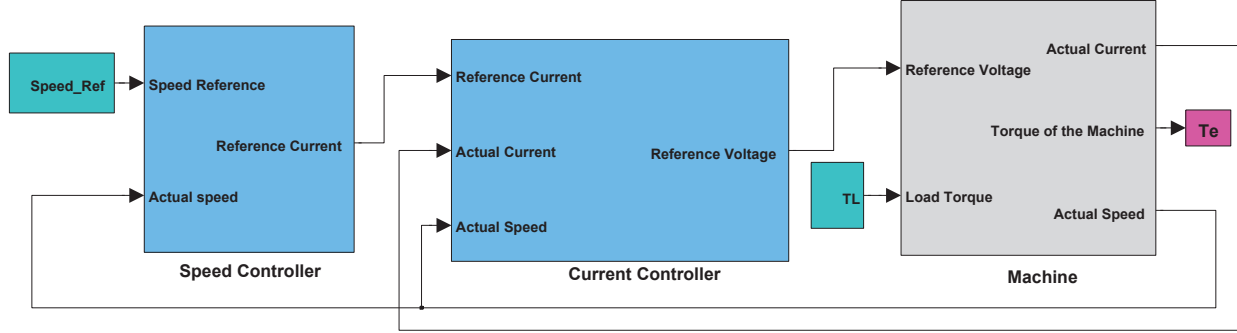


Figure 2.1: General configuration of the control system of PMSM

### 2.2.1 Modeling electrical part of PMSM

According to the PMSM circuits and theories, [6] the general representation of stator voltage can be given as in (2.1)

$$u_s = R_s i_s + \frac{d\psi_s}{dt}. \quad (2.1)$$

and the total flux can be given as depicted in (2.2).

$$\begin{aligned} \psi_s &= \psi_\delta + \psi_{s\lambda} \\ &= \underbrace{(L_m i_s + \psi_m)}_{\psi_\delta} + L_{s\lambda} i_s \\ &= L_s i_s + \psi_m \end{aligned} \quad (2.2)$$

Where  $u_s$  is stator phase voltage,  $R_s$  is the resistance of the machine winding,  $i_s$  is the stator current,  $\psi_s$  is the total flux linkage,  $\psi_\delta$  is the air gap flux linkage,  $\psi_{s\lambda}$  is the leakage flux linkage,  $L_m$  is mutual inductance,  $\psi_m$  is the magnetic flux linkage,  $L_{s\lambda}$  is the leakage inductance and  $L_s$  is the total stator inductance.

### 2.2.2 Modeling PMSM in $\alpha\beta$ -system

The stator voltage and total flux in  $\alpha\beta$ -system can be represented in (2.3) and (2.4) respectively.

$$\underline{u}_s^s = R_s \underline{i}_s^s + \frac{d\underline{\psi}_s^s}{dt} \quad (2.3)$$

$$\begin{aligned} \underline{\psi}_s^s &= \underline{\psi}_{s\lambda}^s + \underline{\psi}_\delta^s \\ &= L_{s\lambda} \underline{i}_s^s + L_m \underline{i}_s^s + \Psi_m e^{j\phi_r} \\ &= L_s \underline{i}_s^s + \Psi_m e^{j\phi_r} \end{aligned} \quad (2.4)$$

The subscript (s) shows the stator reference frame, the superscript (s) shows the stationary  $\alpha\beta$  frame and  $\Psi_m$  is the flux of the permanent magnet and  $\phi_r$  is the rotor position of the machine when the rotor is alligned with phaseA of the machine.

Now, when (2.4) is derivated, (2.5) is obtained.

$$\frac{d\underline{\psi}^s}{dt} = L_s \frac{d\underline{i}_s^s}{dt} + j\omega_r \Psi_m e^{j\phi_r} \quad (2.5)$$

And putting (2.5) in (2.3) hence eliminating  $\frac{d\underline{\psi}^s}{dt}$ , we can further expand the stator voltage equation in  $\alpha\beta$  system as shown in (2.6).

$$\underline{u}_s^s = R_s \underline{i}_s^s + L_s \frac{d\underline{i}_s^s}{dt} + j\omega_r \Psi_m e^{j\phi_r} \quad (2.6)$$

Equation (2.6) can be represented in a circuit as shown in Fig.2.2 [7].

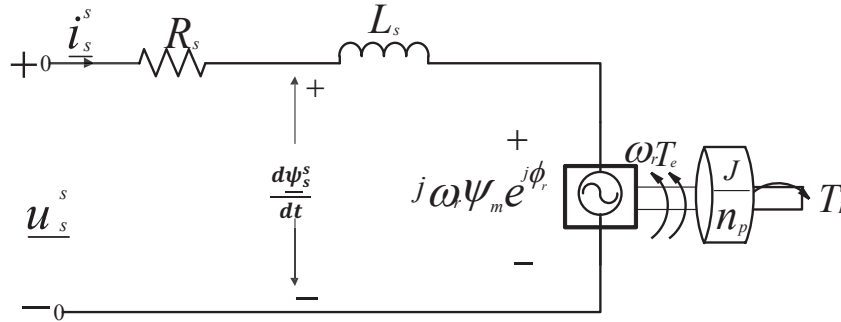


Figure 2.2: Stator voltage circuit showing steps from voltage to torque production

From Fig.2.2 above, the shaft power,  $P_e$  can be given as shown in (2.7).

$$P_e = \frac{3}{2K^2} \text{Re}\{j\omega_r \underline{\psi}_m^s \underline{i}_s^{s*}\} \quad (2.7)$$

where K is the scaling constant.

and the magnetic flux linkage is given by

$$\underline{\psi}_m^s = \underline{\psi}^s - L_s \underline{i}_s^s \quad (2.8)$$

Putting (2.8) in (2.7) we obtain (2.9)

$$P_e = -\frac{3\omega_r}{2K^2} \text{Im}\{\underline{\psi}_s^s \underline{i}_s^{s*}\} \quad (2.9)$$

Finally electrodynamic torque,  $T_e$  can therefore be given as in (2.10).

$$T_e = \frac{P_e}{\Omega_r} = \frac{3n_p P_e}{\omega_r} = \frac{3n_p \omega_r}{2\omega_r K^2} \text{Im}\{\underline{\psi}_s^s \underline{i}_s^{s*}\} = \frac{3n_p}{2K^2} \text{Im}\{\underline{\psi}_s^s \underline{i}_s^{s*}\} \quad (2.10)$$

Here amplitude invariant scaling is assumed, so  $K = 1$  (for peak values) and  $\omega_r$  is the electrical rotor speed,  $n_p$  is the number of pole pairs and  $\Omega_r$  is the mechanical rotor speed.

### 2.2.3 Modeling mechanical part of the PMSM

When the machine is connected to a flywheel of moment of inertia  $J$ , and external load torque  $T_L$  is applied to the flywheel, the speed torque relationship can be given as in (2.11), where,  $\Omega_r$  is the mechanical rotor speed and  $T_e$  is the electrodynamic torque of the machine.

$$J \frac{d\Omega_r}{dt} = T_e - T_L \quad (2.11)$$

The mechanical rotor speed,  $\Omega_r$  can further be defined by (2.12).

$$\Omega_r = \frac{\omega_r}{n_p} \quad (2.12)$$

From (2.10), if we take the imaginary part, we obtain (2.13)

$$T_e = \frac{3n_p}{2} \text{Im}\{\underline{\psi}_s^s i_s^{s*}\} = \frac{3n_p}{2} (\psi_{s\alpha} i_{s\beta} - \psi_{s\beta} i_{s\alpha}) \quad (2.13)$$

where  $\psi_{s\alpha}$  is the real part of the stator flux and  $\psi_{s\beta}$  is the imaginary part of the  $(\alpha\beta)$  stator flux.

Also, if we replace  $\Omega_r$  from (2.11) by (2.12), we further get (2.14)

$$\frac{J}{n_p} \frac{d\omega_r}{dt} = T_e - T_L \quad (2.14)$$

Also, electrical rotor speed,  $\omega_r$  and mechanical rotor position,  $\Phi_r$  can be given in (2.15) and (2.16) respectively

$$\frac{d\phi_r}{dt} = \omega_r \quad (2.15)$$

$$\Phi_r = \frac{\phi_r}{n_p} \quad (2.16)$$

Where  $\phi_r$  is the rotor electrical position.

Alternatively, electrodynamic torque can be given as in (2.17)

$$T_e = \frac{3n_p}{2} \text{Im}\{\underline{\psi}_s^{s*} i_s^s\} \quad (2.17)$$

If we replace  $\underline{i}_s^s$  for (2.18) in (2.17)

$$\underline{i}_s^s = \frac{\psi^s - \Psi_m e^{j\phi_r}}{L_s} \quad (2.18)$$

and after some few manipulations, finally we get (2.19)

$$\begin{aligned} T_e &= \frac{3n_p}{2L_s} \Psi_m \Psi_s (\cos \phi_r \sin \theta_s - \sin \phi_r \cos \theta_s) \\ &= \frac{3n_p}{2L_s} \Psi_m \Psi_s \sin(\theta_s - \phi_r) \\ &= \frac{3n_p}{2L_s} \Psi_m \Psi_s \sin(\delta) \end{aligned} \quad (2.19)$$

where  $\delta = \theta_s - \phi_r$

### Rotating system (dq) representation

To change from stationary system to rotating system, simply multiply the stationary quantities by  $e^{j\theta_r}$  whereby  $\theta_r$  is the electrical rotor position which is taken to be the dq transformation angle by Park transformation theory [8].

So, multiplying (2.6) by  $e^{j\theta_r}$  to move from stationary to dq rotating quantities, we can obtain the stator voltage in dq as shown in (2.20).

$$\underline{u}_s = R_s \underline{i}_s + L_s \frac{d\underline{i}_s}{dt} + j\omega_r L_s \underline{i}_s + j\omega_r \Psi_m e^{j(\phi_r - \theta_r)} \quad (2.20)$$

Doing the same for (2.17) and performing few steps of manipulations, we finally end up with (2.21) for electrodynamic torque.

$$T_e = \frac{3n_p}{2} \Psi_m (i_{sq} \cos(\phi_r - \theta_r) - i_{sd} \sin(\phi_r - \theta_r)) \quad (2.21)$$

Where,  $\phi_r$  is the rotor electrical position angle. For perfect field orientation,  $\phi_r = \theta_r$ , the rotor flux will be aligned in d- direction [7].

Then stator voltage in component forms,  $u_{sd}$  and  $u_{sq}$  can be represented with (2.22) and (2.23) respectively.

$$u_{sd} = R_s i_{sd} + L_s \frac{di_{sd}}{dt} - \omega_r L_s i_{sq} \quad (2.22)$$

$$u_{sq} = R_s i_{sq} + L_s \frac{di_{sq}}{dt} + \omega_r L_s i_{sd} + \omega_r \Psi_m \quad (2.23)$$

The component form of stator voltages,  $u_{sd}$  and  $u_{sq}$  can then be represented in circuit form as shown in Fig.2.3 and Fig.2.4 respectively.

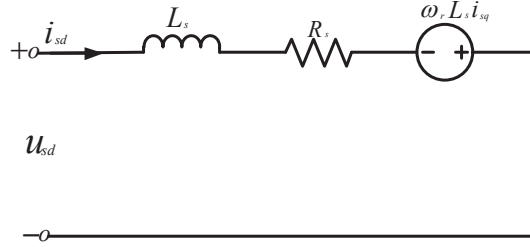


Figure 2.3: d-component stator voltage

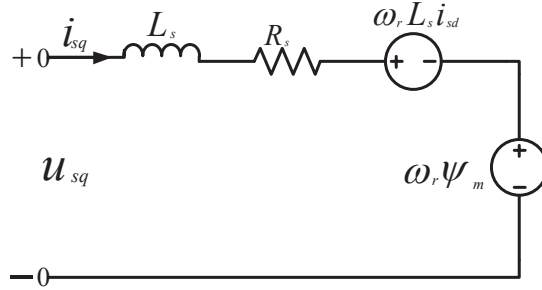


Figure 2.4: q-component stator voltage

The electrodynamic torque can also be transformed to dq form as shown in (2.24)

$$T_e = \frac{3n_p}{2} \Psi_m i_{sq} \quad (2.24)$$

Speed torque relationship and speed position relationship remain to be as in (2.14) and (2.14) respectively.

#### 2.2.4 Current controller design

We are now well informed of the stator voltage which can be further depicted in (2.25).

$$\begin{aligned} \underline{u}_s &= R_s \underline{i}_s + L_s \frac{d\underline{i}_s}{dt} + j\omega_r L_s \underline{i}_s + j\omega_r \Psi_m \\ &= R_s \underline{i}_s + L_s \frac{d\underline{i}_s}{dt} + j\omega_r L_s \underline{i}_s + \underline{E} \end{aligned} \quad (2.25)$$

Here,  $\underline{E}$  has just replaced the term  $j\omega_r \Psi_m$  which is the back-emf of the machine.

Transforming (2.25) to Laplace transform we obtain (2.26)

$$\underline{u}_s - \underline{E} = (sL_s + R_s + j\omega_r L_s) \underline{i}_s \quad (2.26)$$

and finally we get (2.27) which represents the transfer function of the machine,  $G_c(s)$  from voltage to current.

$$\frac{\dot{i}_s}{\underline{u}_s - \underline{E}} = \frac{1}{(sL_s + R_s + j\omega_r L_s)} = G_c(s) \quad (2.27)$$

Representing this transfer function in blocks can be depicted as in Fig.2.5.

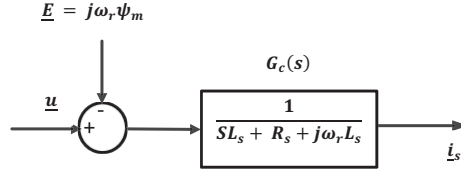


Figure 2.5: Transfer function of the PMS machine

Then adding the estimates of the back-emf,  $(j\omega_r \hat{\Psi}_m)$  de-coupling term,  $(j\omega_r \hat{L}_s \dot{i}_s)$  and the active damping,  $R_a$  to reduce the impact of the back-emf, the resulting voltage will be  $\underline{u}'_s$  as shown in (2.28),

$$\begin{aligned} \underline{u}_s - \underline{E} &= \underline{u}'_s + (j\omega_r \hat{L}_s - R_a) \dot{i}_s + j\omega_r \hat{\Psi}_m \\ &= k_{pc} (\dot{i}_{s,ref} - \dot{i}_s) + \frac{k_{ic}}{s} (\dot{i}_{s,ref} - \dot{i}_s) + (j\omega_r \hat{L}_s - R_a) \dot{i}_s + j\omega_r \hat{\Psi}_m \end{aligned} \quad (2.28)$$

where  $k_{pc}$  and  $k_{ic}$  are proportional and integral gains of the current controller  $F_c(s)$  respectively and  $\dot{i}_{s,ref}$  is the reference current.

Equation (2.28) can be represented in Fig.2.6. The hats indicate the estimated parameters.

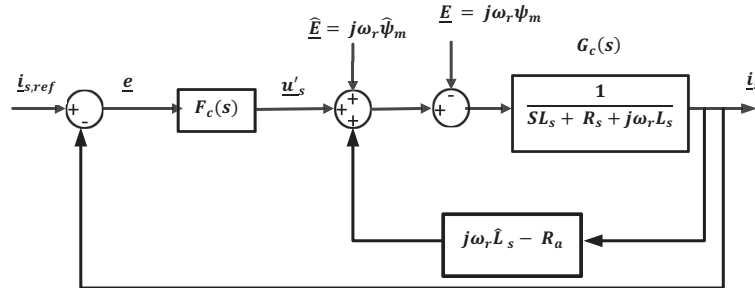


Figure 2.6: Configuration of current control on blocks after addition of estimates

Putting  $\underline{u}_s$  according to (2.26) in (2.28), we obtain (2.29).

$$(sL_s + R_s + j\omega_r L_s) \dot{i}_s + j\omega_r \hat{\Psi}_m = \underline{u}'_s + (j\omega_r \hat{L}_s - R_a) \dot{i}_s + j\omega_r \hat{\Psi}_m \quad (2.29)$$

For perfect parameter estimations, (2.30) is obtained.

$$\begin{aligned} \dot{i}_s &= \frac{1}{(sL_s + R_s + R_a)} \underline{u}'_s \\ &= G'_c(s) \underline{u}'_s \end{aligned} \quad (2.30)$$

Here,  $G'_c(s)$  represents the transfer function the current controller will see.

## How to determine the regulator parameters

By making the closed loop system  $G_{cl}(s)$  to be a first-order low-pass filter [6], then

$$G_{cl}(s) = \frac{\hat{i}_s}{\hat{i}_{s,ref}} = \frac{\alpha_c}{s + \alpha_c} = \frac{\alpha_c/s}{1 + \alpha_c/s} = \frac{F_c(s)G'_c(s)}{1 + F_c(s)G'_c(s)} \quad (2.31)$$

Where  $\alpha_c$  is the bandwidth of the current controller.

Comparing terms in (2.31),  $F_c(s)$  can therefore be given by (2.32).

$$F_c(s) = \frac{\alpha_c}{s} G'_c{}^{-1}(s) = \frac{\alpha_c}{s} \left( s\hat{L}_s + \hat{R}_s + R_a \right) \quad (2.32)$$

This can further be simplified to (2.33).

$$\begin{aligned} F_c(s) &= \alpha_c \hat{L}_s + \frac{\alpha_c(\hat{R}_s + R_a)}{s} \\ &= k_{pc} + \frac{k_{ic}}{s} \end{aligned} \quad (2.33)$$

Now, we need  $G'_c(s)$  to have the same bandwidth as the current regulator, and this can be manipulated as in (2.34).

$$\begin{aligned} G'_c(s) &= \frac{1}{s\hat{L}_s + \hat{R}_s + R_a} \\ &= \frac{1/\hat{L}_s}{s + (\hat{R}_s + R_a)/\hat{L}_s} \\ &= \frac{g\alpha_c}{s + \alpha_c} \end{aligned} \quad (2.34)$$

And finally we get the bandwidth,  $\alpha_c$  of the current controller and the active damping,  $R_a$  as given in (2.35) and (2.36)

$$\alpha_c = \frac{\hat{R}_s + R_a}{\hat{L}_s} \quad (2.35)$$

$$R_a = \alpha_c \hat{L}_s - \hat{R}_s k_{pc} = \alpha_c \hat{L}_s k_{ic} = \alpha_c (\hat{R}_s + R_a) \quad (2.36)$$

## Current reference

From the torque speed relationship in (2.24),  $i_{sq,ref}$  can be obtained as in (2.37)

$$i_{sq,ref} = \frac{2}{3n_p \hat{\Psi}_m} T_{e,ref} \quad (2.37)$$

and since we do not need to produce reactive power, then  $i_{sd,ref}$  is set to zero.



## Voltage saturation and antiwindup

The terminal voltage of the machine can not be made arbitrary large. The upper voltage is set by the capability of the power electronics. However, for larger current reference, the output of the controller exceeds the maximum limit of voltage set. This leads to integral term of the PI controller accumulate the control error during the time of maximum voltage output. This makes the current output to have huge overshoot. To prevent this, an antiwindup branch is introduced to back calculate the reference current to update the integral term of the controller [6].

### 2.2.5 Speed controller design

When designing the speed controller, it is chosen that the current controller is much faster compared to the speed controller [6]. In the same way as done for the current controller, active damping  $B_a$  is introduced to reduce the impact of the disturbances of the load torque  $T_L$  shown in Fig. 2.7.

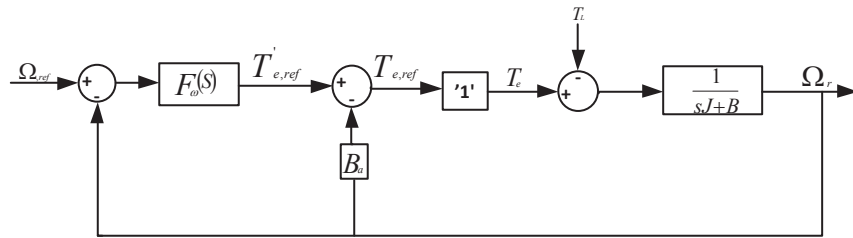


Figure 2.7: Block diagram showing the transfer function of the speed controller

Where  $\Omega_{ref}$  is the mechanical speed reference,  $T_{e,ref}$  is the reference torque,  $B$  is the viscous friction coefficient,  $F_\omega(s)$  is the speed controller and again  $J$  is the moment of inertia of the machine.

The transfer function,  $G'_\omega(s)$  the speed controller will be connected to is given by (2.39)

$$T_{e,ref} = T'_{e,ref} - B_a \Omega_r \quad (2.38)$$

$$\begin{aligned} \implies G'_\omega(s) &= \frac{\Omega_r}{T'_{e,ref}} \\ &= \frac{1}{Js + B + B_a} \end{aligned} \quad (2.39)$$

Therefore Fig. 2.7 can be reduced to Fig. 2.8.

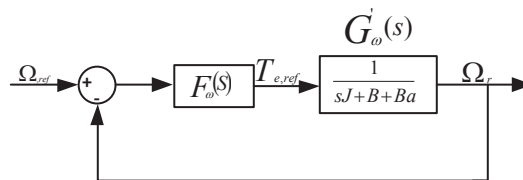


Figure 2.8: Reduced block diagram showing the transfer function to be connected to the speed controller

Also design the speed controller with Internal Model Control (IMC), put the bandwidth of the speed controller to  $\alpha_\omega$

$$\begin{aligned}
G_{cl,\omega}(s) &= \frac{F_\omega(s)G'_\omega(s)}{1 + F_\omega(s)G'_\omega(s)} \\
&= \frac{\alpha_\omega}{s + \alpha_\omega} = \frac{\alpha_\omega/s}{1 + \alpha_\omega/s} \\
\implies \frac{\alpha_\omega}{s} &= F_\omega(s)G'_\omega(s) \\
F_\omega(s) &= \frac{\alpha_\omega}{s}G'_\omega(s) \\
&= \frac{\alpha_\omega}{s}(Js + B + B_a) \\
&= \alpha_\omega J + \frac{\alpha_\omega(B + B_a)}{s} \\
&= K_{p\omega} + \frac{K_{i\omega}}{s} \tag{2.40}
\end{aligned}$$

Where,  $K_{p\omega}$  and  $K_{i\omega}$  are proportional and integral gains of the speed controller respectively. Selecting the active damping,  $B_a$  so that  $G'_\omega(s)$  gets the same bandwidth ( $\alpha_\omega$ ) as the speed controller, and this gives:

$$\begin{aligned}
\alpha_\omega &= \frac{B + B_a}{J} \\
\implies B_a &= \alpha_\omega J - B \\
K_{p\omega} &= \alpha_\omega J \\
K_{i\omega} &= \alpha_\omega(B + B_a) \\
&= \alpha_\omega(B + J\alpha_\omega - B) = J\alpha_\omega^2 \tag{2.41}
\end{aligned}$$

Therefore:

$$T_{e,ref} = \left( K_{p\omega} + \frac{K_{i\omega}}{s} \right) (\Omega_{r,ref} - \Omega_r) - B_a \Omega_r \tag{2.42}$$

## 2.3 Simplorer

Simplorer is a circuit modeling software which is also used in this thesis project. Simplorer, a trademark of Ansys, is a simulation package for electric circuit simulations that allows one to easily and quickly model all components of an application. It can be used to design and model electric, electronic, control and mechanical components [9]. Simplorer has a user friendly graphical interfaces making even complex models easy to define [10]. Due to its ability to inter-link with Maxwell and Simulink, Simplorer was the best choice to be used as the interface engine in the co-simulation of thesis project.

### 2.3.1 Steps of coupling Simulink to Simplorer

The process of coupling Simulink to Simplorer is well explained in the Simplorer11 documentation. Therefore, the explanation of the steps is as per Simplorer11 documentation [11].

The Simplorer model to be connected to Simulink is created and saved independently. Then, Simulink model has to be created but without any AnsoftSFunction. Save the simulink model. In Simplorer model created, add a Simulink component by following the arrows.

(Simplorer Circuit →SubCircuit→Add Simulink Component).

The Simulink interface window will appear where you will have to browse the Simulink model. In that window, add the connection pins you desire to connect the signals to and from Simplorer and Simulink (using the "LinkAssignment" box). Then press the OK button and the Simulink model with the name (MDL) will be imported to Simplorer. Save the Simplorer model with the Simulink model imported.

In Simulink, create an S-Function and give it a special name "AnsoftSFunction". Pressing OK, the SiM2SiM interface window appears. Check the "Read link from information file", then browse to the Simplorer you have created. Link the signals that they appear in the SiM2SiM interface window. If you link the signals, they will appear in the box that is at the bottom of the SiM2SiM window. Then press OK. Resize the AnsoftSFunction block created in Simulink as you want and make the connections to other blocks in Simulink. Save the simulink model. The simulation is started in Simplorer and when simulation is started in Simplorer, Simplorer will run Simulink as well to establish the link and exchange data.

#### **Note:**

Not all versions of Matlab/Simulink can generate this special S-Function with the name of AnsoftSFunction. 64-bit versions are not supported. (The version used in this thesis was R2010b 32-bit)

## 2.4 Maxwell

Maxwell is one of the Ansoft Corporation softwares well known for Finite Element Method modeling. In this project, Maxwell is mainly used to build and analyze the permanent magnet synchronous generator. Maxwell has many features which altogether make analysis of machine models. Models generated in Maxwell can also be inter-linked to Simplorer for co-simulation. It can also make simulation by itself which can make possible to observe the machine parameters and performances.

### 2.4.1 How to build a generator in Maxwell

One can build electric machines using Maxwell in different ways. Although it is possible for someone who is familiar with the software to build models of machines from scratch, it is rather time consuming. However, the process is simplified by letting the RMXprt do the most of the job. RMXprt is a machine model whereby a software user can insert machine design parameters and related information. This is a user friendly interface even for beginners of the software [12].

In the process of inputting the design data in the RMXprt, a user has to specify the dimensions of the stator and rotor of the machine and related parameters such as machine type, number of poles of the machine and control type. Furthermore, a user has to specify the rated parameters such as speed and voltage. A user has also to specify other parameters such as winding, slot, wire, conductors, insulation and some other related parameters [13].

### 2.4.2 Steps of coupling Maxwell to Simplorer

The explanation of the steps of coupling Simplorer with Maxwell is mainly based on [14]. When the generator is completely built in Maxwell and analyzed, then it be prepared for co-simulation with Simplorer. The excitation is previously defined with current sources. In order to use Maxwell model in co-simulation with Simplorer, the user needs to do some modifications on the Maxwell model.

On the Maxwell project tree (be it 2D or 3D), right mouse click on **Model** tab, then click "**Set Symmetry Multiplier**". On the design Setting pop-up window, go to the **Advanced Product Coupling** tab and enable **Transient-Transient** link with Simplorer. This will let Maxwell know that everything linked to rotor position and winding information are to be taken from Simplorer.

Then go to the winding definition under the **Excitation** tab. Right mouse click on **PhaseA**, then select **Properties**. For each winding, you need to enter that you want the current information to be read in Simplorer. Select **External** in the **Type** pull down menu. Make sure that the initial current is 0. Repeat the same operation for **PhaseB** and **PhaseC**.

In Simplorer, add transient cosimulation as shown with these following arrows.  
Simplorer Circuit → SubCircuit → Maxwell Component → Add Transient Cosimulation.

In the **Transient-Transient** coupling window that appears, browse to open the Maxwell project saved before. Maxwell is opened and loads the project. In the **Transient-Transient** coupling window, the project information are loaded. Select the project you modified in Maxwell and in the **Option** tab, select **Pin Description** and click **OK**. Place the component and make the connections.

# Chapter 3

## Modeling

### 3.1 Model of the control system in Simulink

The theory discussed in chapter two is now used to model the control system for the generator.

#### 3.1.1 General machine control arrangement

The general arrangement of the controllers to the machine is as depicted in Fig. 3.1.

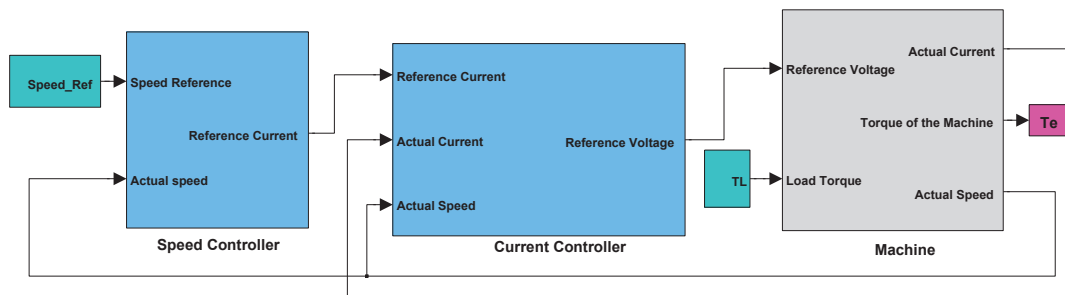


Figure 3.1: General configuration of the machine with control system

The complete machine and its control system was first built in Simulink so as to observe the dynamic behavior of the controller before it was connected to the FEM model.

#### 3.1.2 S-Function of the machine

The first step was to represent the machine in the S-Function as shown in Fig. 3.2.

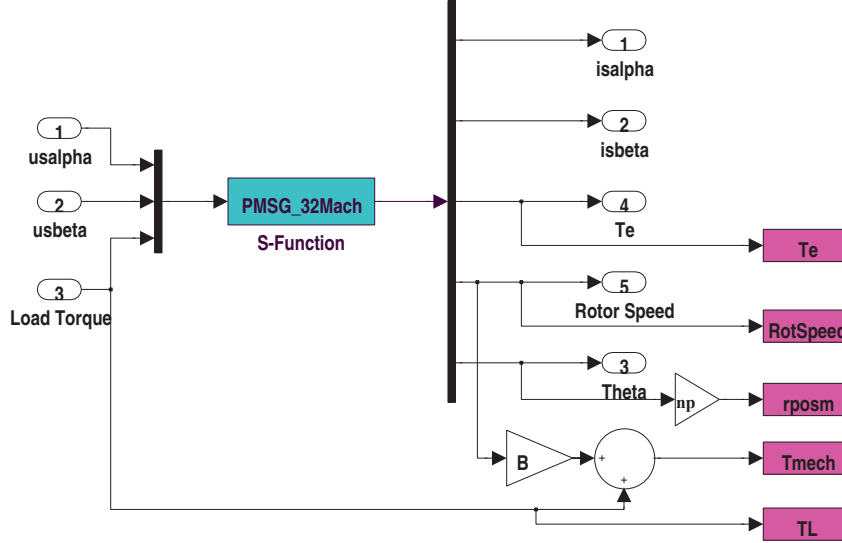


Figure 3.2: S-Function of the machine

The inputs to the S-Functions are the voltage generated by the controller. The outputs of the S-Function are currents, electrodynamic torque, rotor speed and position which are taken as feedback to the controller to generate the reference voltage to the machine. The representation of the machine is done in the motor reference system. Since the generator is what intended to be controlled, then, the only changes from the motor reference system is the direction of the current. In this representation, the current will be negative, giving negative torque and hence negative power generated.

### 3.1.3 Current control

The current of the machine is measured and transformed from the abc three phase quantities to dq quantities. The main reason for this transfer is to get dc quantities which when implemented in PI controllers can allow the gains of the controllers to increase as much as possible so as to eliminate any error introduced in the system. When using ac quantities with specific frequency, say 50Hz in the controllers, the gains of the controllers are limited to certain values and therefore there is a possibility not to eliminate the error introduced in the system.

Fig. 3.3 shows the general current control configuration. It takes in the actual current from the machine then compares it with the reference current which is set by the speed controller to be discussed later. If the reference current and the actual current are not equal, error  $e$  is generated and input to the PI regulator of the current controller.

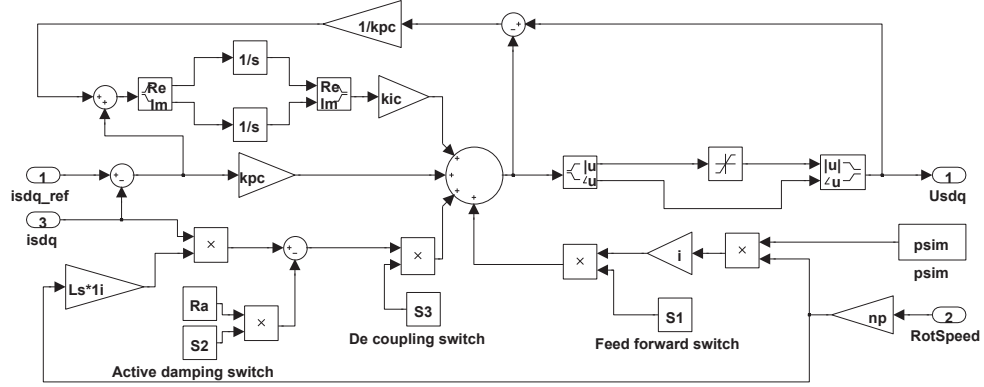


Figure 3.3: Current control configuration of the system

In the integral part of the current controller as shown in Fig. 3.3, a saturation block is introduced to limit the voltage to the rated value. Due to a voltage limiter, if it happens the current controller produces higher voltage than the rated value, then integral part of the current controller accumulates high value which will interfere the controlability of the current controller. To remove this setback, a branch called anti-windup is added to the controller.

### 3.1.4 Current limiter

There is a need to design a current limiter so as to protect the generator winding. If no current limitation is introduced, there is a risk of drawing a huge current compared to the rating of the machine when a large load is connected which can lead to burning the winding of the machine. Fig. 3.4 represents a Simulink model of the current limiter in the control system.

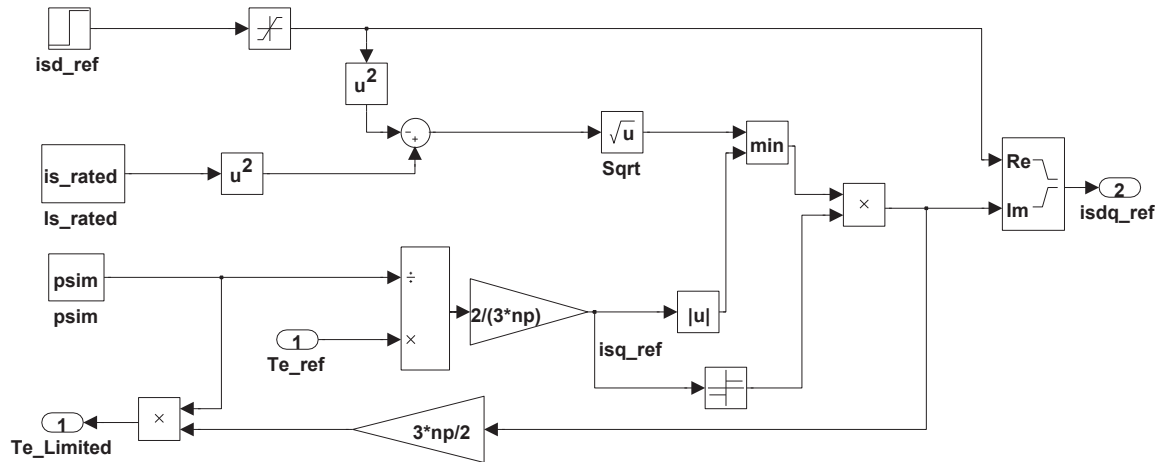


Figure 3.4: Current limitation model of the control system

### 3.1.5 Speed control

The inputs to the speed controller are the reference speed and mechanical torque. It further gets back the actual speed of the machine which is compared to the reference speed provided. If there is a difference between these speeds, the error is input to the PI regulator which operates to remove the error. The speed controller then

produces the reference current as output which is one of the inputs to the current controller as discussed before in current controller part. Fig. 3.5 shows the details of the speed controller model.

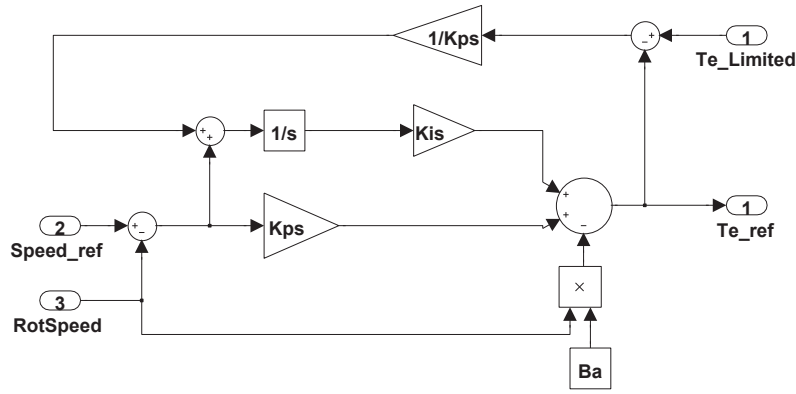


Figure 3.5: Speed control of the system

### 3.1.6 Complete model of the control system

Finally, the complete model of the control system can be seen on Fig. 3.6.

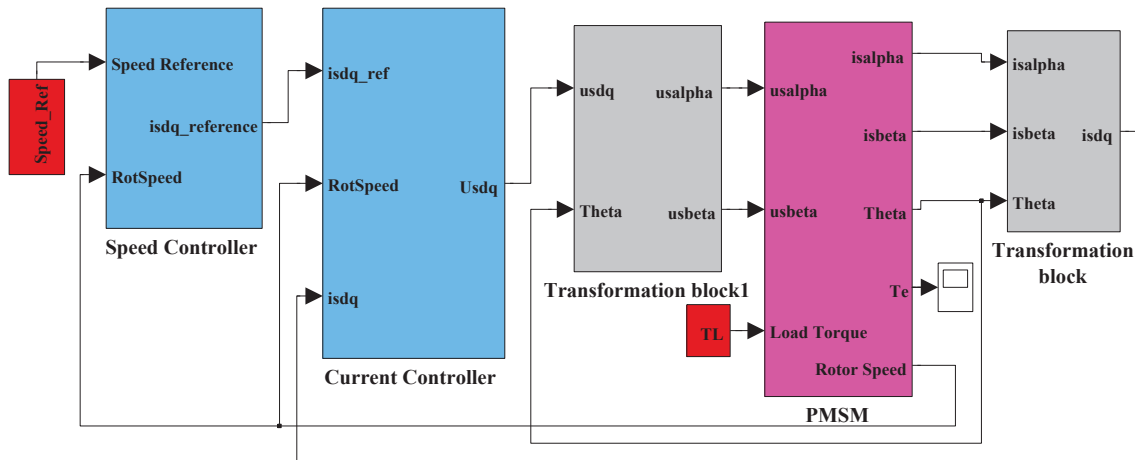


Figure 3.6: Complete model of the control system configuration

## 3.2 Coupling of control system with Simplorer and verification

After verifying the controller with the simulations which are shown in simulation chapter, the next step was to link the control system to Simplorer. This was done by replacing the machine in the Simulink S-function with a generic PMSM in Simplorer. The PMSM and the voltage sources which will be linked to Simulink voltages were placed in Simplorer work sheet. The Simulink control system was then imported to Simplorer as shown in the complete coupled model of Simplorer PMSM and Simulink control system in Fig. 3.7.



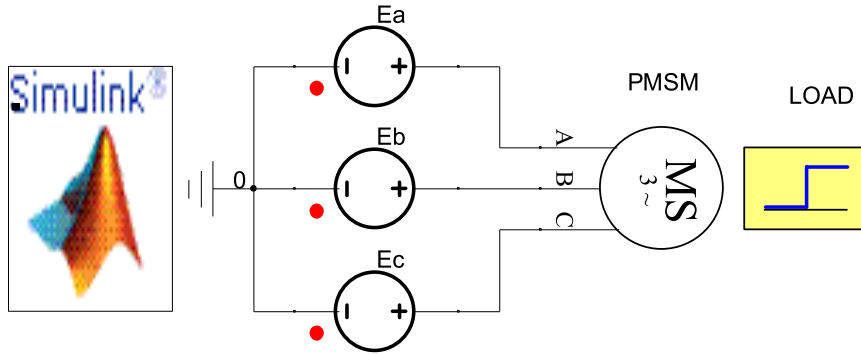


Figure 3.7: Coupling of Simulink control system and Simplorer PMSM

In Simulink, the SiM2SiM interface link is generated by a special S-function named AnsoftSFunction which links the signals from the PMSM in Simplorer to Simulink control system. The interface platform generated in Simulink is as shown in Fig. 3.8.

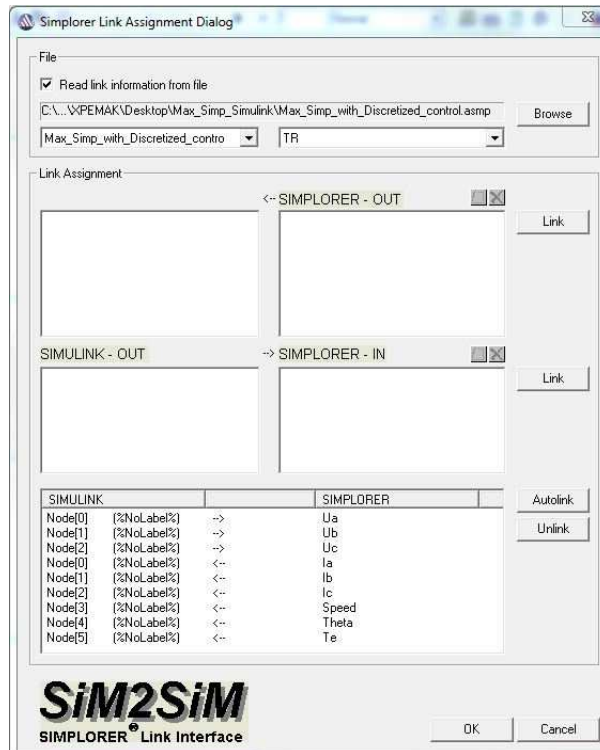


Figure 3.8: Simulink to Simplorer interface platform

When all signals are linked in the SiM2SiM link interface, AnsoftSfunction block is generated in Simulink. The Block shows the corresponding pins which are to be linked to Simulink and from Simplorer as shown in the linked control system to Simplorer, Fig. 3.9. This enables signals from Simplorer to be linked to Simulink and signals from Simulink to be linked to Simplorer.

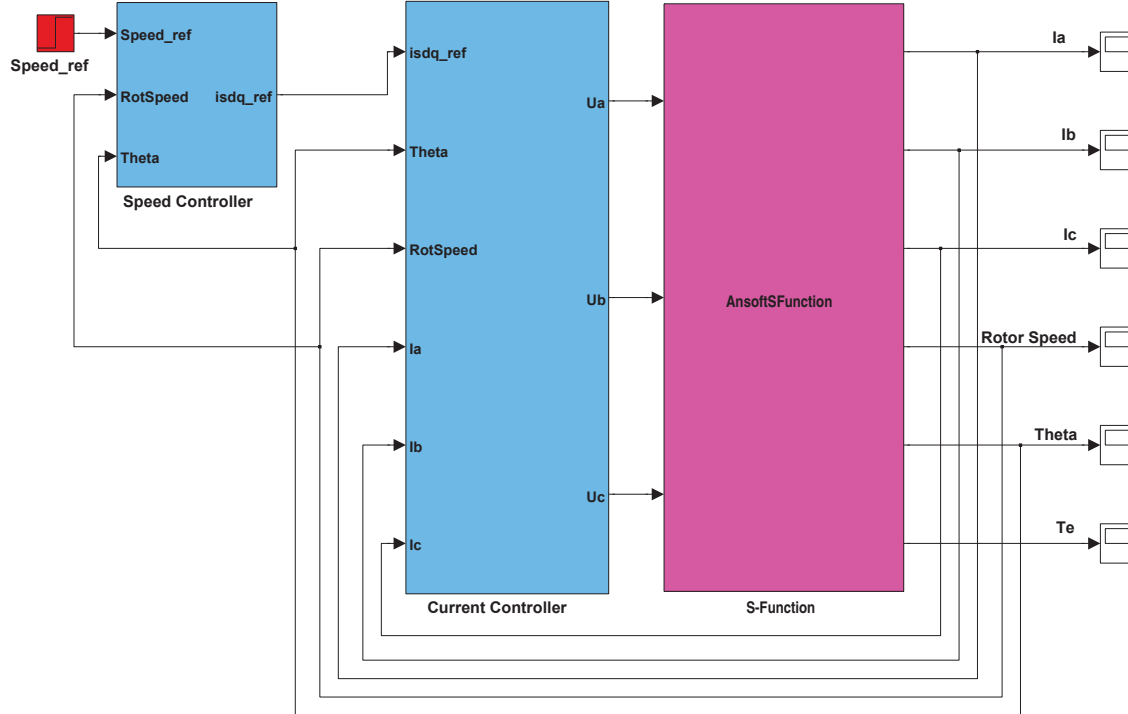


Figure 3.9: AnsoftSFunction block linking Simulink control system to Simplorer PMSM

When all signals are linked, simulation is started in Simplorer. Simplorer calls and hence runs Simulink which provides reference voltage for the machine. In turn, when the machine in Simplorer runs, it provides signals for the control system. The signals from the machine in Simplorer are speed, armature current, and rotor position which are linked to Simulink. These signals are passed to the Simulink control system via the SiM2SiM link interface. The control system uses the signals from the machine to compare with the reference signals to generate the reference voltages which are passed to the PMSM through the SiM2SiM link interface again.

### 3.3 Finite Element Method model of the PMSG

The generator for wind power application is modeled using Finite Element Method. The type of the machine used in the RMxprt is the variable speed Synchronous machine with 100 rpm as rated speed, 200 V as rated voltage and 32 poles. The rated power of the machine is 120kW.

Other parameters and dimensions of the machine were collected from the machine description manual provided. The parameters and dimensions were input to the RMxprt for the Adjustable Speed Synchronous Machine model in Maxwell. The parameters which were input to the RMxprt model of the machine are categorized in following tables.

Table 3.1 shows the general parameters of the machine to be used in the RMxprt so as to develop the FEM machine model.

Table 3.1: General parameters of the machine model

Name	Value and Units
Machine Type	Adjust-Speed Synchronous Machine
Number of poles	32
Rotor position	Outer Rotor
Reference speed	100 rpm
Control type	AC
Circuit type	Y3

The stator and its related parameters and dimensions were input as shown in Table 3.2.

Table 3.2: Stator parameters

Name	Value and Units
Outer diameter	1600 mm
Inner diameter	1300 mm
Length	140 mm
Stacking factor	0.95
Steel type	M19_24G
Number of slots	168
Slot type	4
Skew width	0

The stator slot design was done as shown on Fig. 3.10 and the related dimensions are shown in Table 3.3.

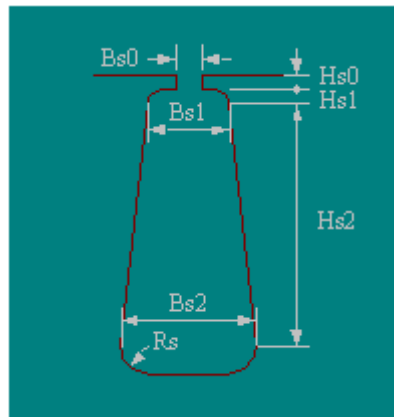


Figure 3.10: Slot design of the machine

Table 3.3: Slot design

Name	Value and Units
Hs0	2.5 mm
Hs1	0 mm
Hs2	76 mm
Bs0	4 mm
Bs1	11.3 mm
Bs2	11.3 mm
Slot type	4
Skew width	0

After the designing of the stator slot, the winding calculations were done so as to fit in the slots and hence be able to withstand the rated voltage and carry the rated current. The information for the winding is shown in Table 3.4.

Table 3.4: Winding

Name	Value and Units
Winding layers	1
Winding type	Whole Coiled
Parallel branches	4
Conductor per slot	17
Number of strands	4
Wire wrap	0
Wire size	Diameter: 2 mm

Last but not the least was to input given information for the rotor. The rotor for this machine is in the outer position. The main reason of the machine to be outer rotor type is to support the design of the distributed bearings which in turn increases the mechanical rigidness of the generator which is the intended feature of the machine [15]. The Table 3.5 shows the parameters of the rotor of the machine.

Table 3.5: Rotor parameters

Name	Value and Units
Outer diameter	1798 mm
Inner diameter	1650 mm
Length	140 mm
Stacking factor	0.95
Steel type	M19_24G
Pole type	4

This machine is excited by the permanent magnets to increase the efficiency of the machine. The absence of winding in the rotor reduces the copper loss in the machine hence improves efficiency. These magnets are placed in the outer rotor to provide

the intended excitation of the machine. Table 3.6 shows the magnetic type used in this construction and other related magnetic information.

*Table 3.6: Magnetic information*

<b>Name</b>	<b>Value and Units</b>
Embrance	0.7
Offset	0
Magnet type	XG196/96 mm
Magnet thickness	22 mm

The RMXprt is now ready, but before it is simulated, it has to be provided with some further machine specifications which are shown in Table 3.7. These are the ratings of the machine and the load type to be connected.

*Table 3.7: Other machine specifications*

<b>Name</b>	<b>Value and Units</b>
Operating type	Generator
Load type	Infinity bus
Rated Output Power	120 kW
Rated Voltage	200 V
Rated Speed	100 rpm
Operating temperature	75 ° C

Finally, the complete RMXprt model of the generator is shown in Fig. 3.11.

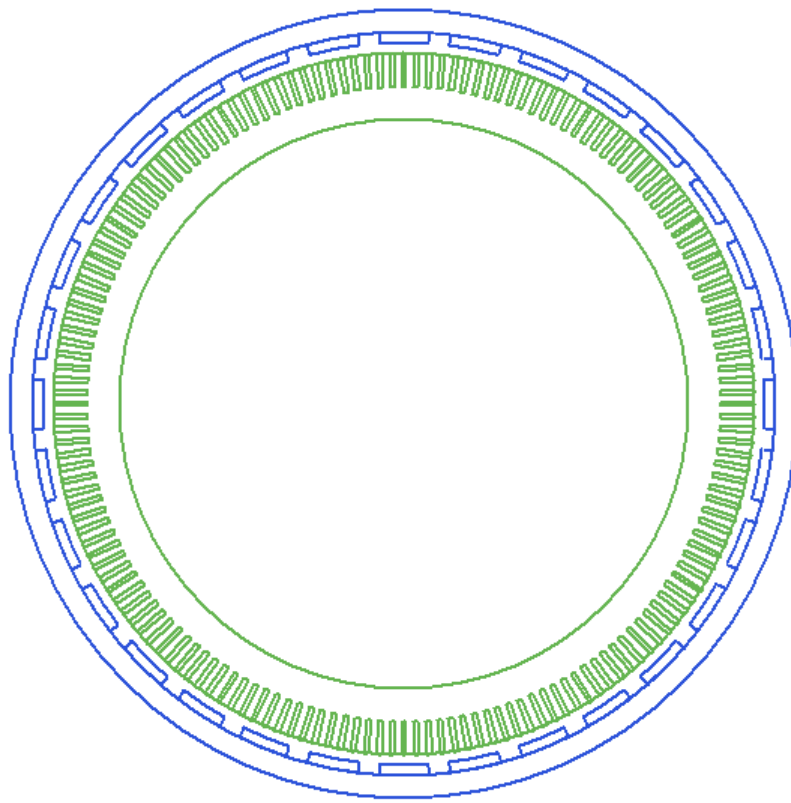


*Figure 3.11: RMxprt model of the machine*

When the RMxprt model was analysed, general generator design data sheets were obtained as shown in Appendix A. The design data sheets indicate different parameters and material used in the machine design. Furthermore, some graphs showing different behaviour of parameters of the machine are generated by the software as shown in Appendix B.

The next step was to export the model to the 2D model. This was done by undergoing few steps on Maxwell software, which has the functionality of generating 2D model from the RMxprt model. This functionality generates all necessary information required for the 2D transient analysis. The exported 2D model is shown in Fig. 3.12.

When the model is exported to 2D or 3D model, it takes reasonably long time to solve the model. To reduce this setback, the software tries to divide the RMxprt model to the smallest possible symetries. So when converting to 2D or 3D, it only computes solution for only one of the symetries. For this case, the machine has been divided into four equal parts and only one part is represented on 2D model as shown on Fig. 3.12.

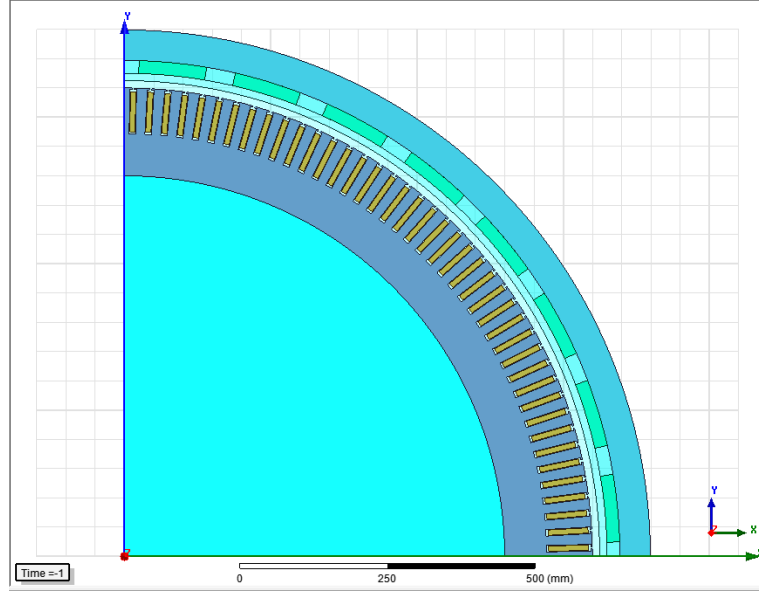


Figure 3.12: 2D model of the machine

### 3.4 Coupling of FEM model with Simplorer and verification

In order to verify the behaviour of the FEM model, it was coupled to a Simplorer circuit. A constant mechanical speed source was applied to the generator modeled in Maxwell through a speed source component with a symbol  $\omega$ . Fig. 3.13 refers to the FEM model connected to a simple circuit in Simplorer. A line to line fault switch is also included in the circuit to see how the machine behaves during fault condition. A fault activator activates the fault switch which then activates the fault through a fault resistor  $R_{\text{fault}}$  at a desired time instant. Simulations for this connection are shown in the Simulation chapter.

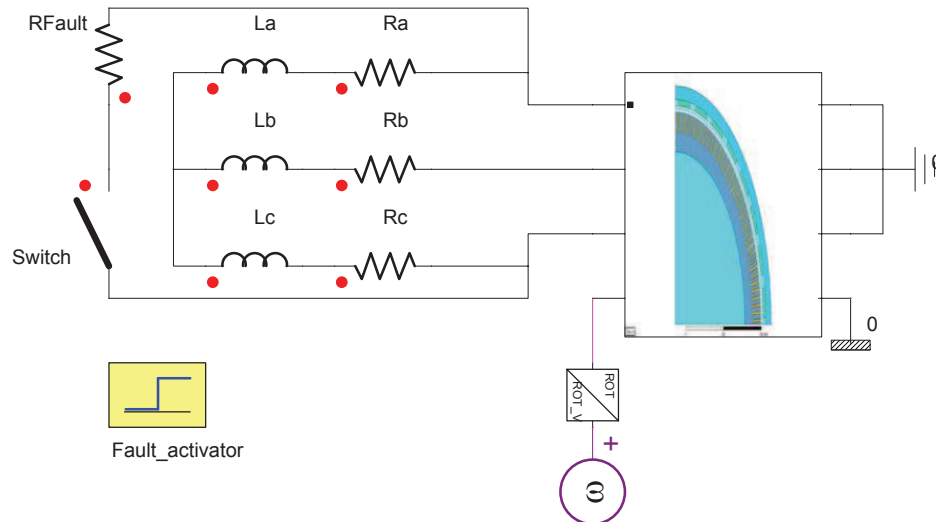


Figure 3.13: Coupling of FEM model with Simplorer

### 3.5 Embedding FEM model to Simulink control system using Simplorer

After building and verifying the FEM model when coupled with Simplorer, and verification of the control system in Simulink coupled to Simplorer, the next step was to couple these two models (FEM model and control system model). Simplorer was used to facilitate this process. The FEM model was modified and prepared to be exported and communicated to Simplorer as explained in the theory in chapter two. FEM model was then imported to Simplorer. The next procedure was to add the Simulink control system model to Simplorer as well. Armature currents come from the three voltage sources (EA.I, EB.I, EC.I), and speed (FEA1.OMEGA), rotor position (FEA1.PHI) and torque (FEA1.TORQUE) comes from the generator model (FEM) and are linked to the Simulink control system model (MDL). These signals are needed by the Simulink control system model to generate control signals for the generator. The controller compares the machine values with the reference values and generates volt-age signals to the machine. The complete coupled/embedded model can be seen in Fig. 3.14.

Mechanical dynamics of the machine were modeled in Simplorer using blocks. Electrodynamic torque of the machine,  $T_e$  was input to a (CONST) block and load torque,  $T_L$  was input to a step block. An integral block, (I) gets in the difference between  $T_e$  and  $T_L$  divided by the moment of inertia of the rotating mass. The integral block generates the speed which is input to the machine through the speed source labeled  $\omega$  as seen in Fig. 3.14.

A line to line fault is as well included in the circuit set-up. The fault activator activates the fault switch which then activates the fault through a fault resistor, Rfault as seen in Fig. 3.14.

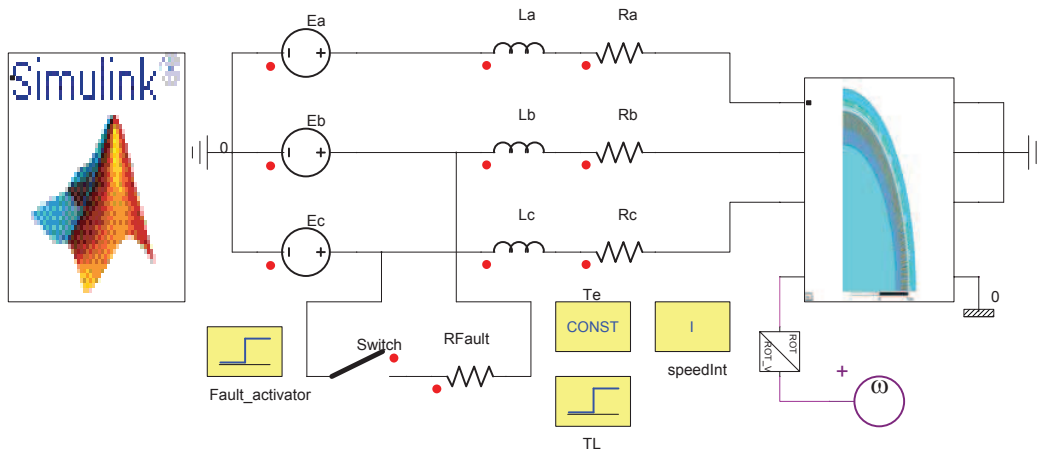


Figure 3.14: Coupling of FEA with Simulink using Simplorer



# Chapter 4

## Simulation

### 4.1 Simulation approach

As it has been pointed out from chapter one that, the intention of the project is to co-simulate a permanent magnet synchronous machine modeled in Maxwell with a controller modeled in Simulink, Simplorer used as interfacing software. The simulation process has been approached in four steps. The first step deals with simulations which verify the performance of the controller. In this step, both controller and machine are modeled in Simulink. The second step is the co-simulation of the PMSM modeled in Simplorer with the controller modeled in Simulink. In this step, simulations verify coupling together Simulink and Simplorer. The third step deals with simulations which verify the performances of the FEM model. The FEM model is coupled to Simplorer and simulations are performed. This part also verifies co-simulation between Maxwell and Simplorer. The final step is the co-simulation of PMSG modeled in Maxwell and controller modeled in Simulink with Simplorer used as an interface platform.

The main simulation parameter to look on is torque. However, to understand better the performances of the machine and the controller, other parameters are taken into account. These parameters are rotor speed, armature currents and voltages of the machine.

### 4.2 Simulation of PMSM and controller in Simulink

In this simulation, machine and controllers were arranged and set up as shown in Fig. 3.6. The simulations were done by setting the speed reference to the controller which was set to 100rpm, which is the rated value of the machine. At 1.5s, a load torque of -2kNm was applied to the machine.

Fig. 4.1 shows three phase stator voltage waveforms at no load and when the load torque of -2kNm is applied to the machine at 1.5s.

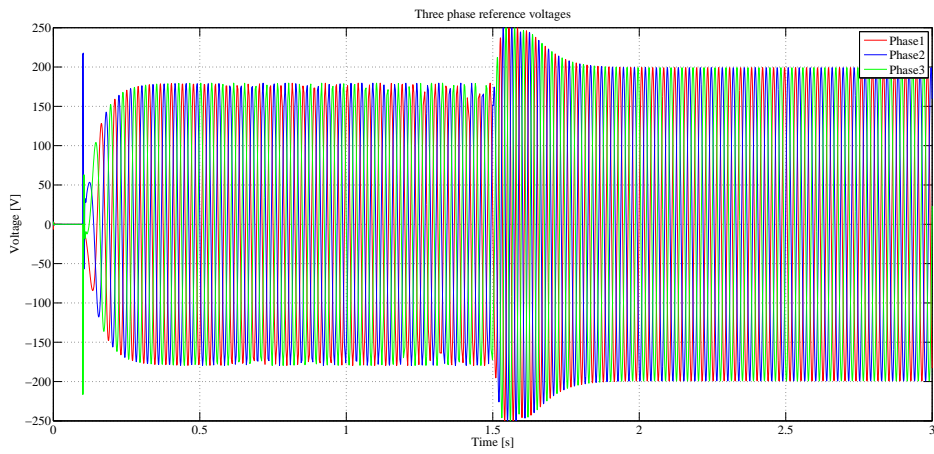


Figure 4.1: Simulink simulation showing three phase stator voltages at rated speed

To observe the behaviour of the three phase stator voltages when a load torque is applied to the machine, a zoomed simulation is shown in Fig. 4.2.

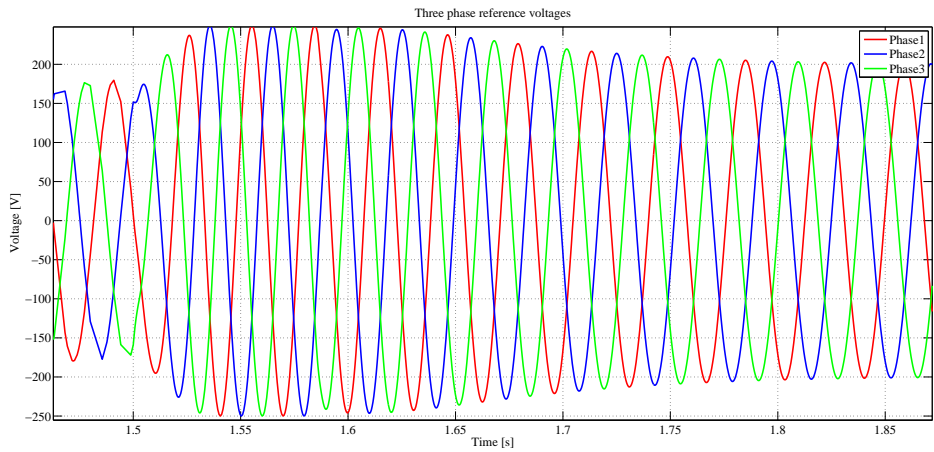


Figure 4.2: Simulink simulation showing zoom of three phase stator voltages when a load torque is applied

Fig. 4.3 indicates how the speed controller operates to keep the rotor speed of the machine to the reference value at the beginning of the simulation and when the load torque is applied.

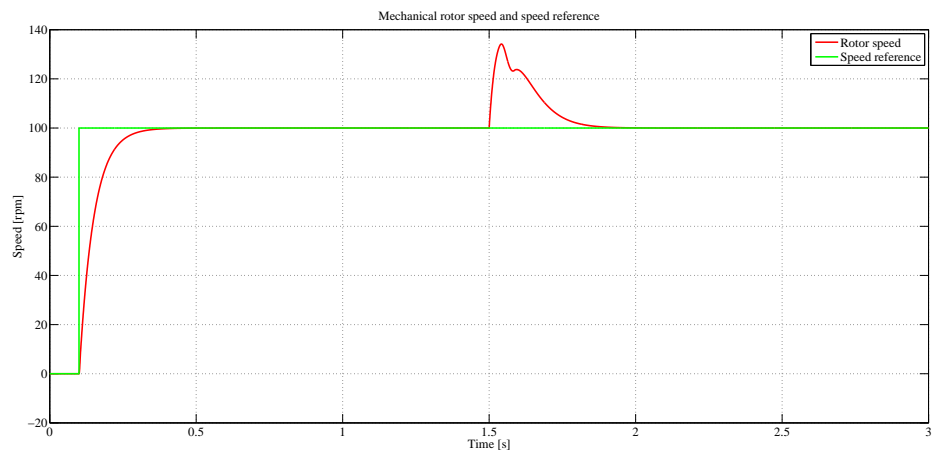


Figure 4.3: Simulink simulation showing rotor speed of the machine and speed reference

Fig. 4.4 shows the machine current waveforms at no load and when the load torque of  $-2\text{kNm}$  is applied to the machine at 1.5s.

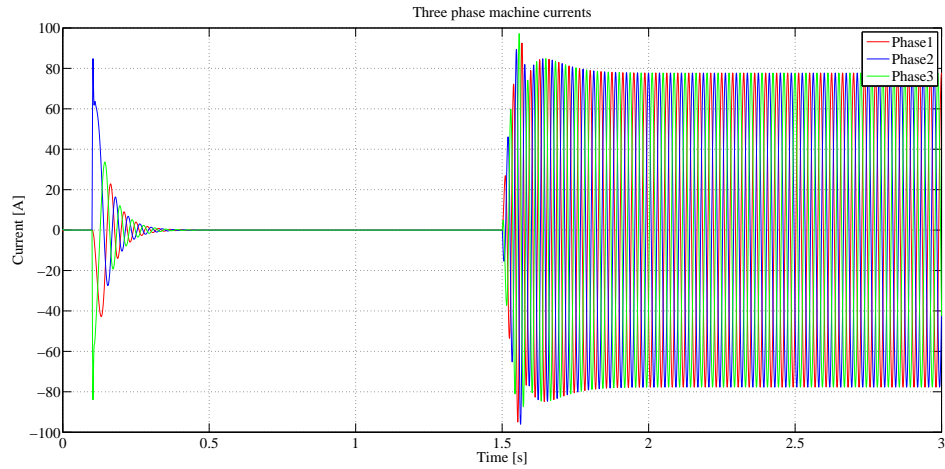


Figure 4.4: Simulink simulation showing three phase armature currents of the machine at rated speed

To observe the behaviour of the three phase currents of the machine when a load torque is applied, a zoomed simulation is shown in Fig. 4.5.

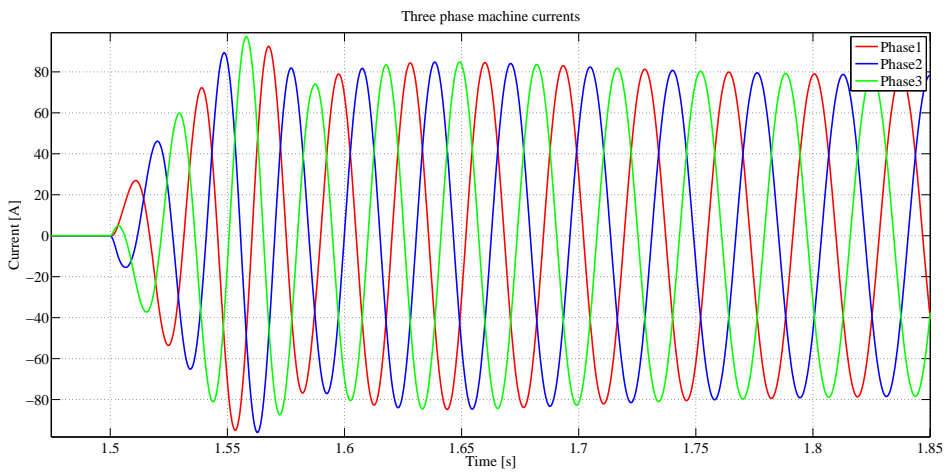


Figure 4.5: Simulink simulation showing zoom of three phase armature currents of the machine when load torque is applied

Similarly, Fig. 4.6 refers to the response of the electrodynamic torque of the machine when a load torque of  $-2\text{kNm}$  is applied to the machine at 1.5s.

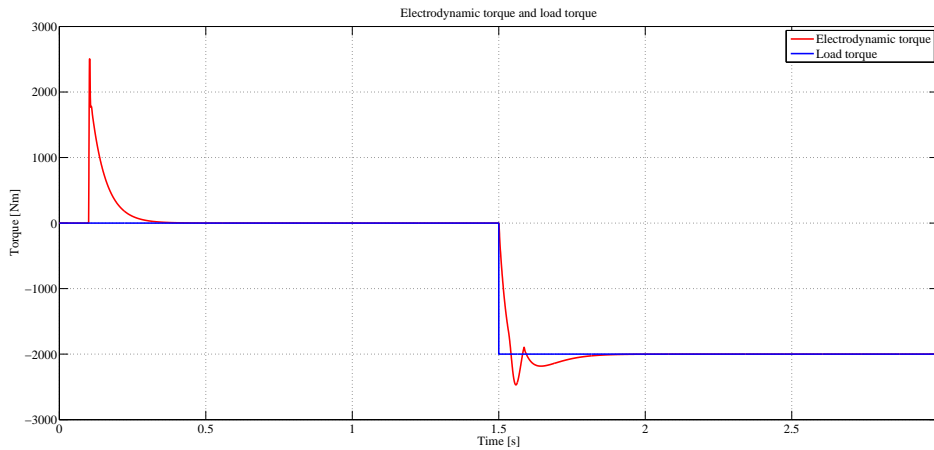


Figure 4.6: Simulink simulation showing electrodynamic torque of the machine at rated speed

### 4.3 Co-simulation of PMSM in Simplorer and controller in Simulink

The next step as explained before was to replace the machine that was modeled in Simulink with an equivalent generic machine modeled in Simplorer. The control system in Simulink was imported to Simplorer and connected as shown in Fig. 3.7. The reference speed of 100rpm was provided to the controller in Simulink. After then, the simulation was started in Simplorer which then calls Simulink control system. After the simulation coming to steady state at 1.5s, load torque of  $-2\text{kNm}$  was applied to the machine. The intention of this simulation step is to verify co-simulation between Simulink and Simplorer. The responses were as shown in the following figures.

The response of the three phase stator voltages of the Simulink-Simplorer co-simulation of the machine can be observed in Fig. 4.7.

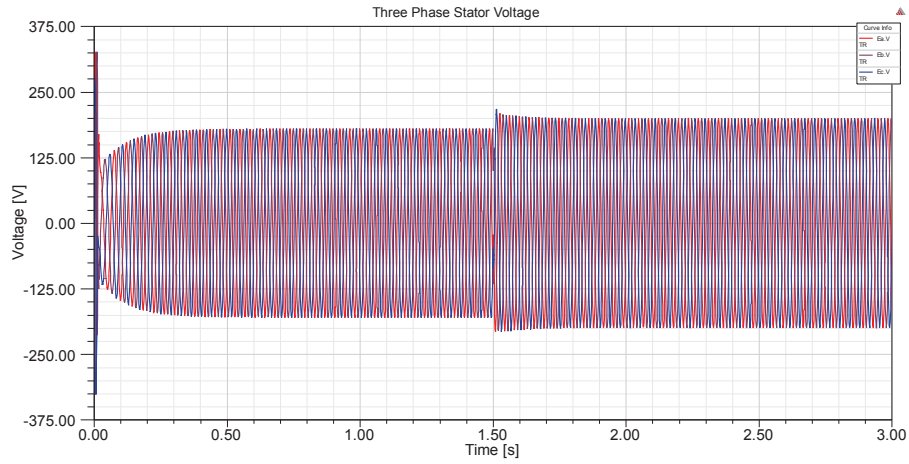


Figure 4.7: Simplorer-Simulink co-simulation showing three phase stator voltages

To observe the behaviour of the three phase stator voltages when a load torque is applied to the machine, a zoomed simulation is shown in Fig. 4.8.

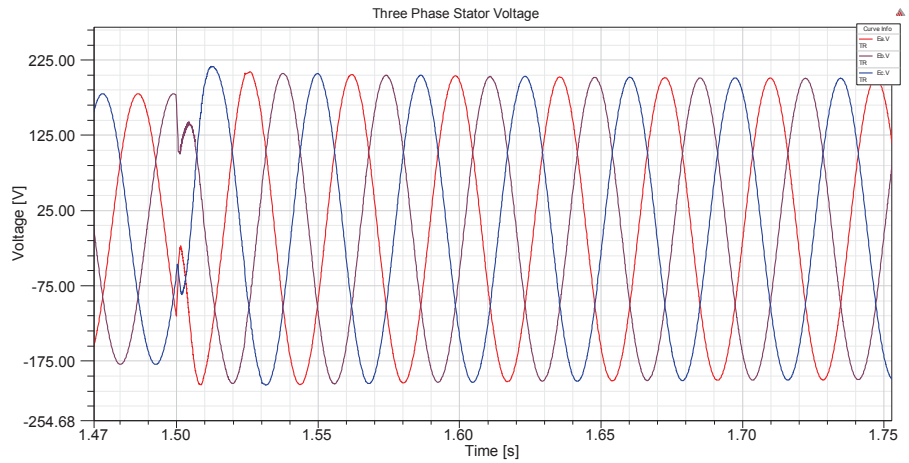


Figure 4.8: Simplorer-Simulink co-simulation showing zoom of three phase voltages when load torque is applied

The response of the rotor speed of the Simulink-Simplorer co-simulation can be seen in Fig. 4.9 at no load and when load torque is applied to the machine.

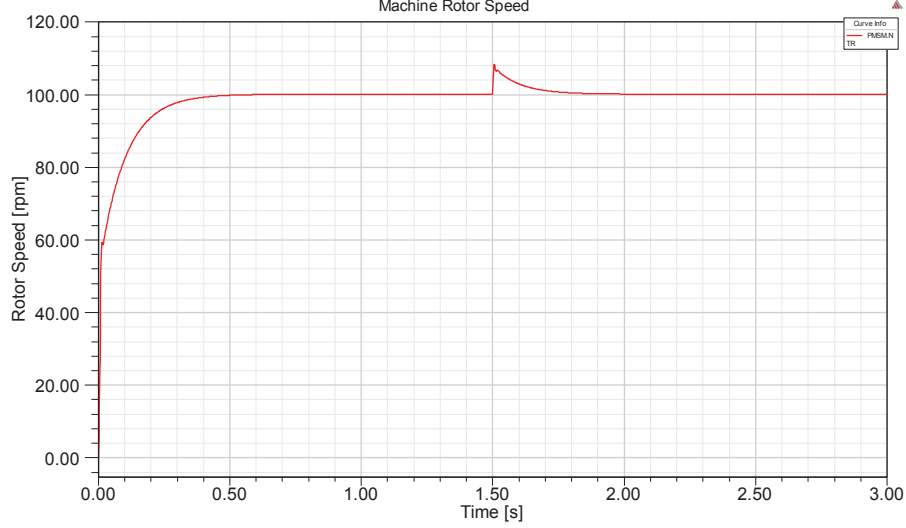


Figure 4.9: Simplorer-Simulink co-simulation showing rotor speed of the PMSM

The response of the three phase armature current of the Simulink-Simplorer co-simulation can be observed in Fig. 4.10.

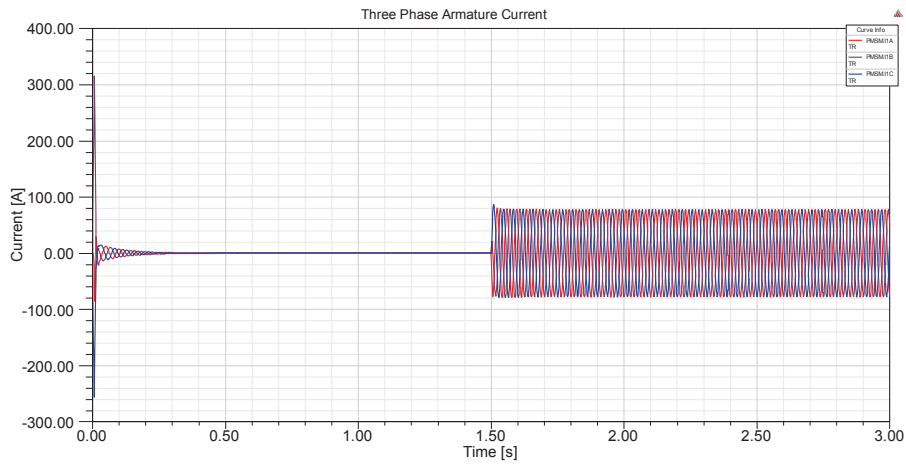


Figure 4.10: Simplorer-Simulink simulation showing three phase armature currents

To observe the behaviour of the three phase current of the machine when a load torque is applied, a zoomed simulation is shown in Fig. 4.11.

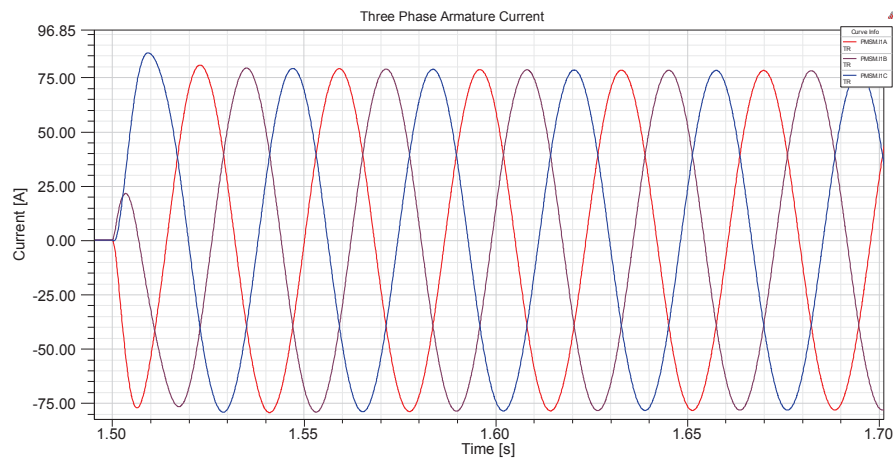


Figure 4.11: Simplorer-Simulink simulation showing zoom of three phase armature currents when load torque is applied

Fig. 4.12 shows the response of the electrodynamic torque of the Simulink-Simplorer co-simulation of the machine at no load and when load torque is applied to the machine.

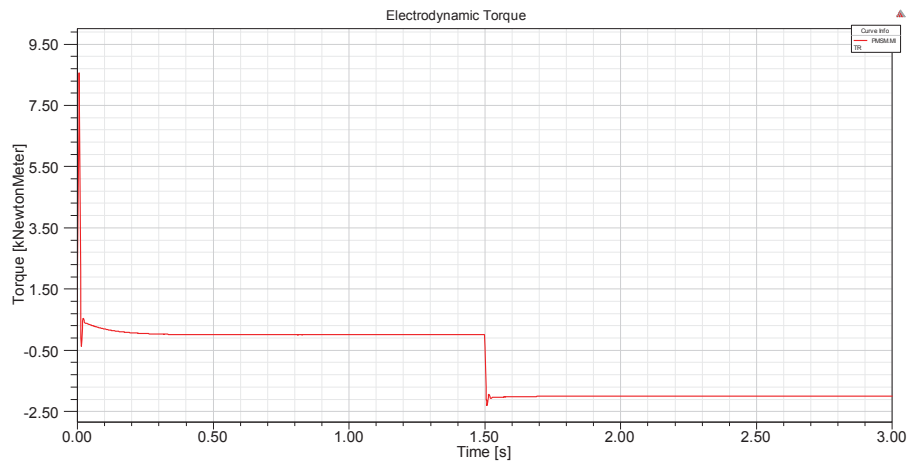


Figure 4.12: Simplorer-Simulink co-simulation showing electrodynamic torque of the machine

## 4.4 Co-simulation of FEM model and Simplorer

In order to verify the performance and behaviour of the generator modeled using FEM in Maxwell, the FEM model was imported in Simplorer and connected to a simple circuit as shown in Fig. 3.13. A constant mechanical speed of 100rpm which is the rated speed of the machine was then applied to the FEM model. This made the machine to rotate and induce back-emf in windings of the machine as shown in simulation Fig. 4.13.

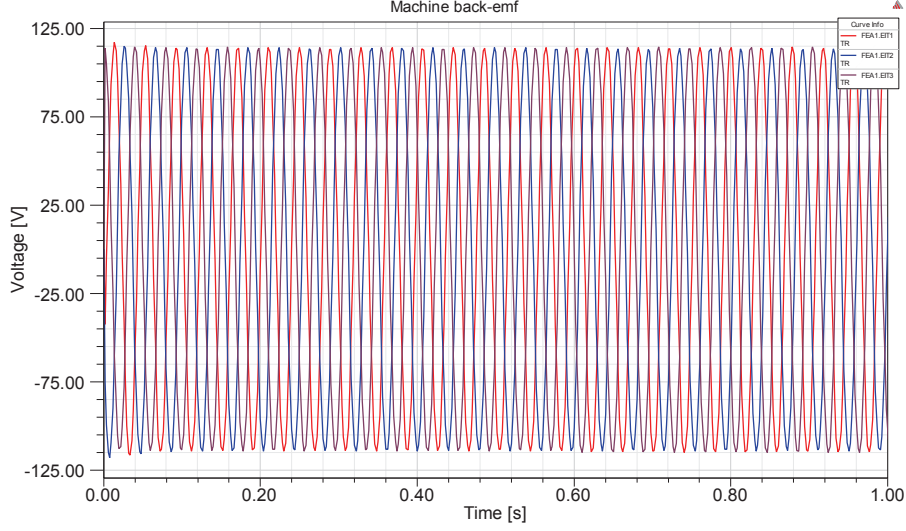


Figure 4.13: Induced back-emf in the windings of the machine model

Fig. 4.14 is a zoom part of the back-emf simulation shown in Fig. 4.13.

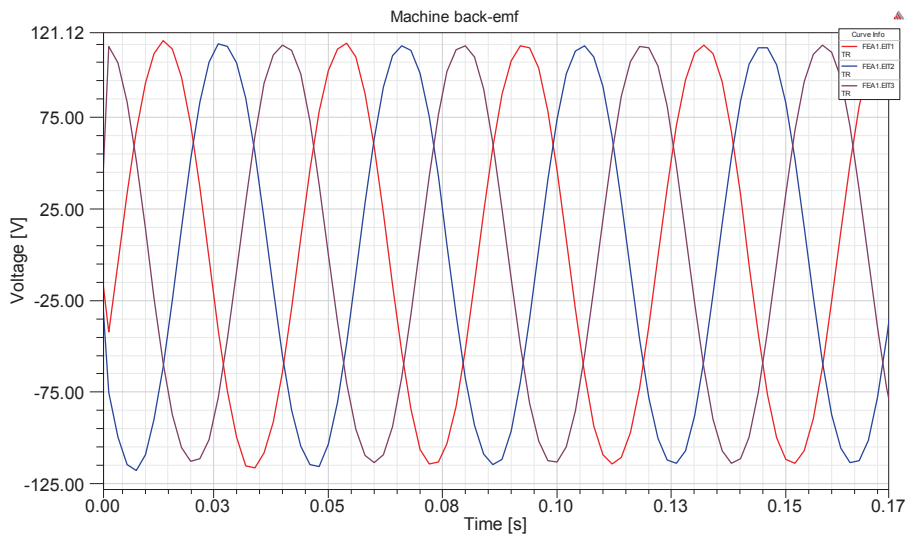


Figure 4.14: Zoom of the induced back-emf in the windings of the machine model

Fig. 4.15 indicates the three phase currents of the machine. At 0.6s, a line to line fault is introduced in the system as shown in Fig. 3.13. The response of the currents of the machine to the fault can be seen in Fig. 4.15 from time 0.6s.



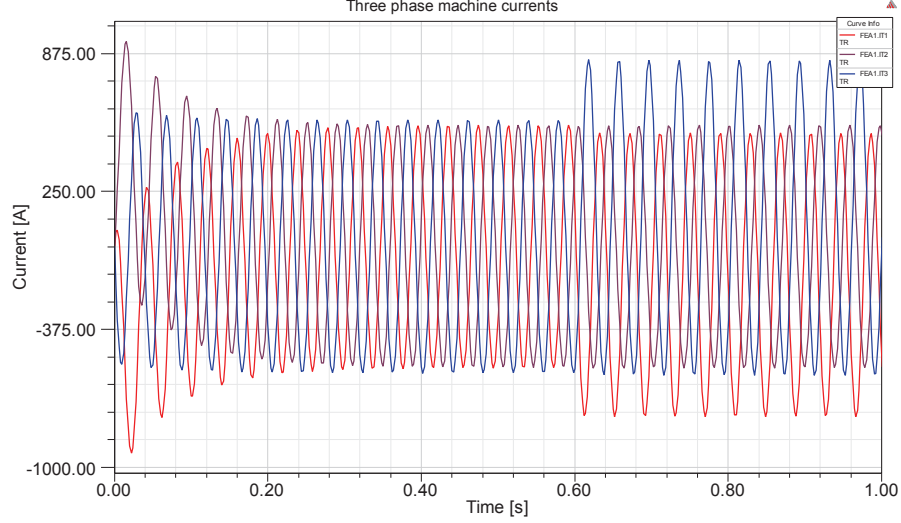


Figure 4.15: Three phase currents of the machine when driven by mechanical speed and the response to a line to line fault

Fig. 4.16 shows a zoom part of the three phase machine currents response when a line to line fault is introduced in the system.

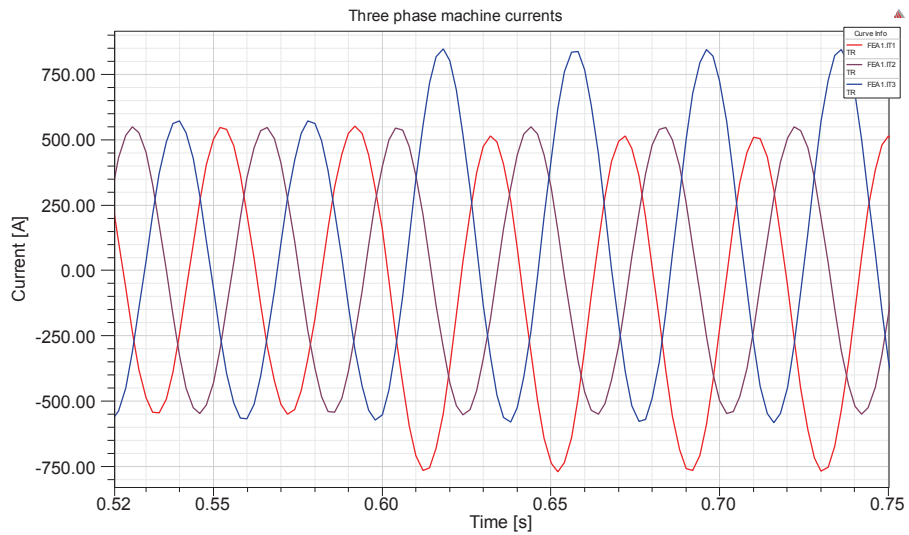


Figure 4.16: Zoom of the three phase currents of the machine when driven by mechanical speed and the response to a line to line fault

Similarly, Fig. 4.17 indicates the torque response of the machine when driven with mechanical speed and also shows the response of the machine electrodynamic torque when a line to line fault is introduced in the system.

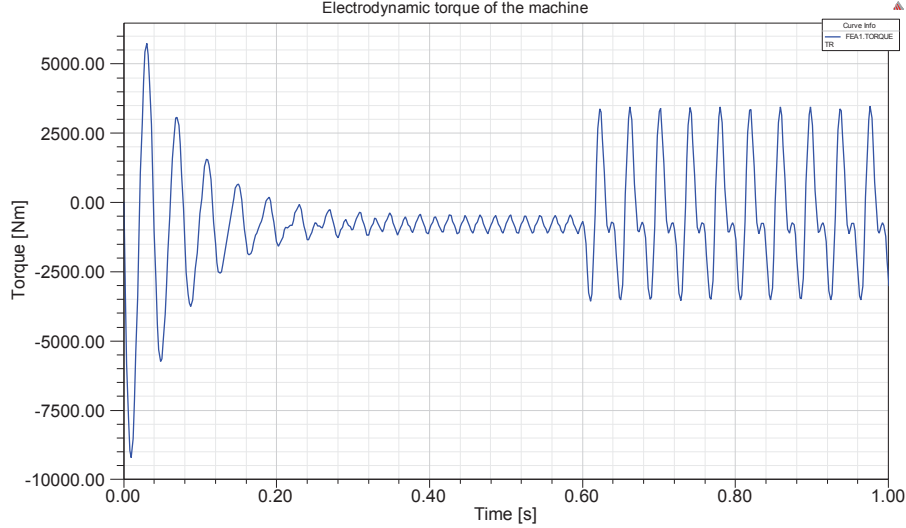


Figure 4.17: Electrodynamic torque of the machine when driven by mechanical speed and the response to a line to line fault

## 4.5 Co-Simulations of embedded FEM model in Simulink control system using Simplorer

After verifying the performance of controller in Simulink, controller in Simulink coupled to Simplorer and verification of performance of the FEM model when coupled to Simplorer; the final step was to extend these ideas to embed the FEM model to Simulink control system using Simplorer. The circuit set-up for this step was done as shown in Fig. 3.14. A speed reference of 100rpm is set in the controller in Simulink. At 0.6s a load torque of -2kNm is applied to the machine. Finally, a line to line fault is introduced in the system at 1.5s.

Fig. 4.18 shows the back-emf induced in the machine windings at no load, when a load torque is applied and when the line to line fault is introduced in the system.

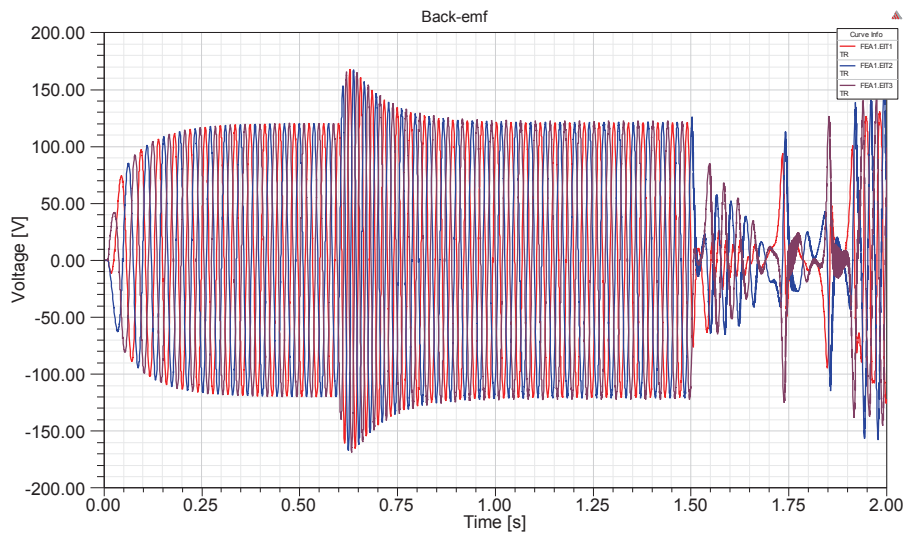


Figure 4.18: Co-simulation showing back-emf induced in the machine windings

To better observe the behaviour of the induced back-emf in the windings before and after load torque is introduced, a zoom part of the back-emf simulation is shown in Fig. 4.19.

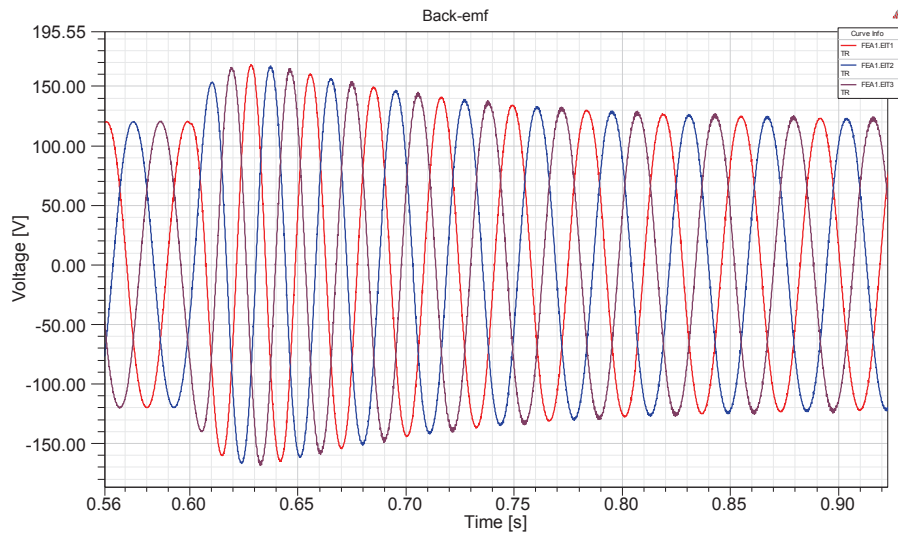


Figure 4.19: Co-simulation showing zoom of back-emf induced in the machine windings when a load torque is applied

The response of the rotor speed of the machine can be seen in Fig. 4.20.

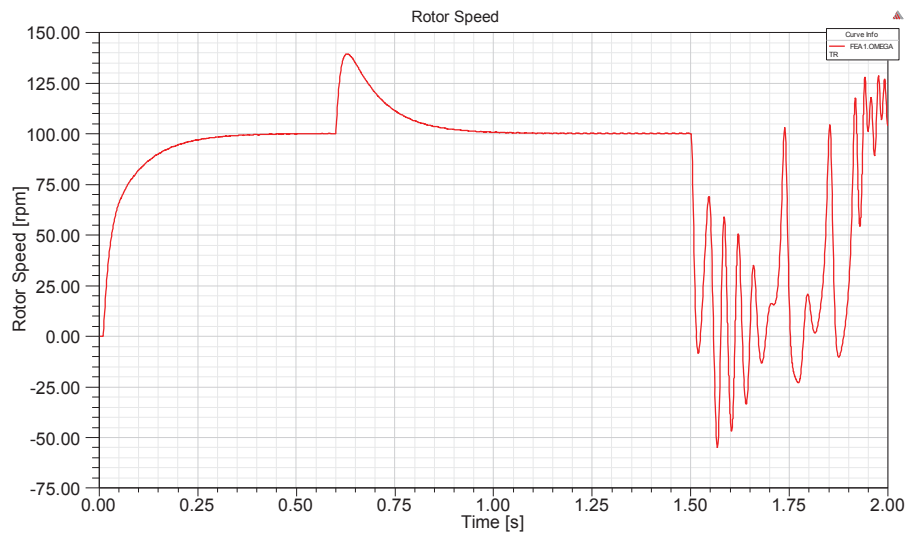


Figure 4.20: Co-simulation showing rotor speed of the machine

Fig. 4.21 shows the behaviour of the three phase currents of the machine at no load, when load torque is applied and when the line to line fault is introduced in the system.

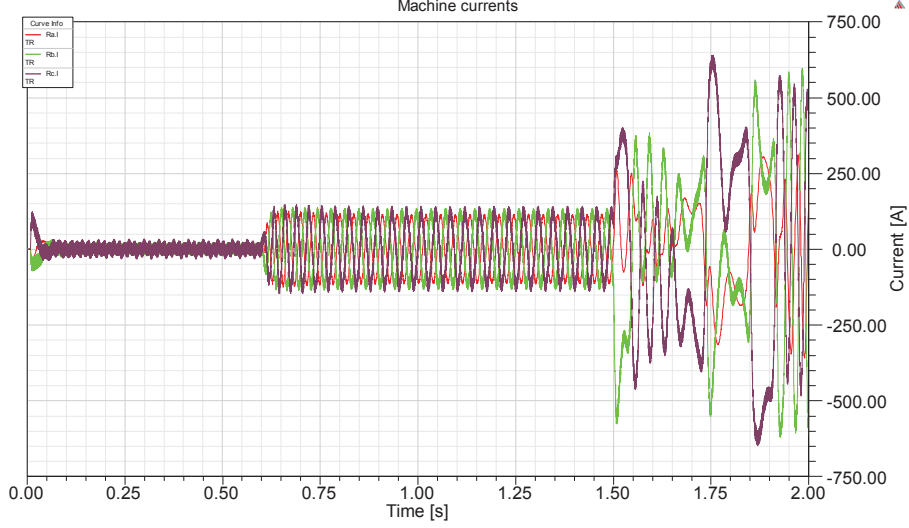


Figure 4.21: Co-simulation showing three phase currents of the machine

To closely observe the response of the three phase currents of the machine, a zoom part of the three phase currents is as seen in Fig. 4.22.

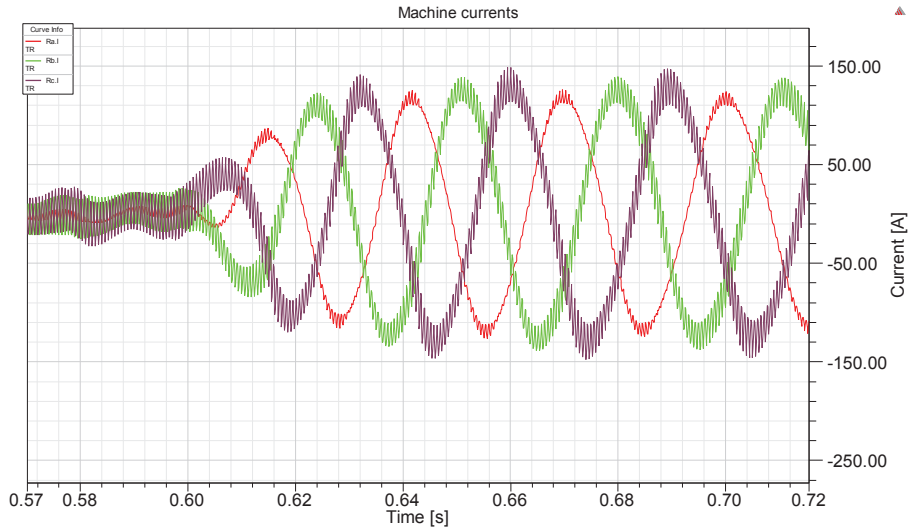


Figure 4.22: Co-simulation showing zoom of three phase currents of the machine when a load torque is applied

Similarly, comparison of electrodynamic torque of the machine (FEA1.TORQUE), load torque (Tm.VAL) and reference torque from the controller (MDL1.Te\_ref) can be seen in the simulation Fig. 4.23.

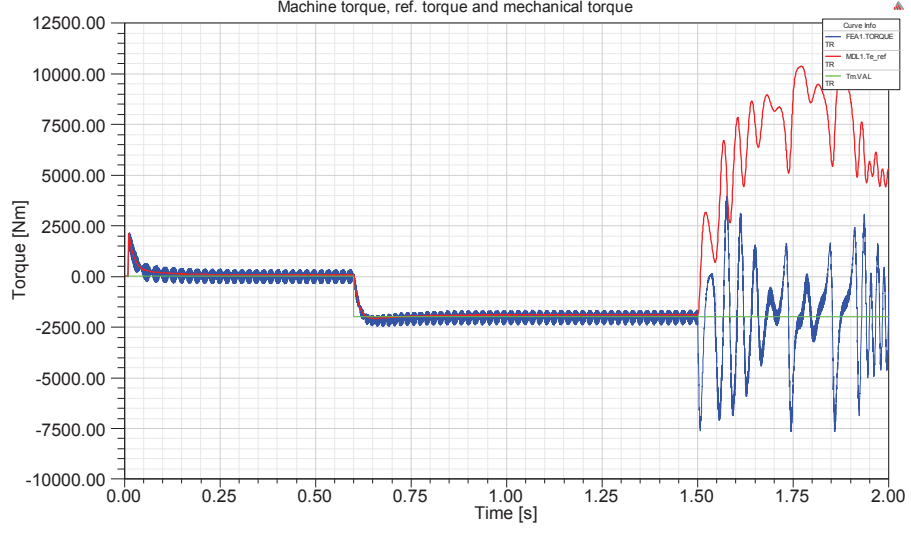


Figure 4.23: Co-simulation showing electrodynamic torque of the machine, reference torque and load torque



# Chapter 5

## Analysis, conclusion, recommendation and future work

### 5.1 Analysis of simulation results

#### 5.1.1 Analysis and verification of the controller performance

Simulink simulations represent an example of the first-order harmonic model within dynamic simulation. In this simulation step, it can be seen from the waveforms that the controller does its part to set the rotor speed of the machine to the reference value. For this case, the rotor speed of the machine responds to the controller and goes to 100rpm which is the reference value set at the beginning of the simulation. Also when a load torque of -2kNm is applied at 1.5s, the rotor speed of the machine tries to increase but the controller reacts to put it to the reference value as seen in Fig. 4.3.

Currents are also controlled and hence controlling the torque of the machine at no load and when a load torque is applied at 1.5s as seen in Fig. 4.4 and Fig. 4.6 respectively. The frequency of the voltages and currents generated is 26.67Hz at steady state conditions as seen in the zoomed simulations Fig. 4.2 and Fig. 4.5 respectively.

#### 5.1.2 Analysis and verification of co-simulation between Simulink and Simplorer

Looking on Simplorer-Simulink co-simulations, it was verified that coupling between Simplorer and Simulink is possible. The behavior looks the same with simulations in Simulink. The controller does its part to keep the rotor speed of the machine to the reference value as seen in Fig. 4.9. Currents are also controlled and hence controlling the torque of the machine at no load and when a load torque of -2kNm is applied at 1.5s as seen in Fig. 4.10 and Fig. 4.12 respectively. The frequency of the voltages and currents generated is 26.67Hz at steady state conditions as seen in the zoomed simulations Fig. 4.8 and Fig. 4.11 respectively.

### 5.1.3 Analysis and verification of FEM model performance

The simulations were done to verify the performance of the FEM model. At the rated speed of 100rpm which is applied to the machine as shown in Fig. 3.13, back-emf is induced in the machine windings as seen on Fig. 4.13. The frequency of the induced back-emf is 26.67Hz as can be observed in the zoomed back-emf simulation waveforms in Fig. 4.14. The machine model also produces currents which further result to electrodynamic torque as seen in Fig. 4.15 and Fig. 4.17 respectively. The currents and torque oscillate at the beginning of simulation because there is no controller for the machine. The torque damps with time, but still at steady state has smaller oscillations compared to oscillations at the beginning.

At 0.6s, a line to line fault is activated in the system. The machine responds to the fault as the two phases currents increase as seen in Fig. 4.15 and Fig. 4.16. This results to huge oscillation of the torque as seen in Fig. 4.17.

This simulation part verifies that the FEM model is performing as expected and it is also possible to co-simulate when couple with Simplorer.

### 5.1.4 Analysis of embedded FEM model in Simulink controller

Finally comes the Maxwell-Simplorer-Simulink co-simulation. A rated speed reference of 100rpm was applied to the controller in Simulink. As a result of the action of the controller, back-emf is induced in the machine windings as seen in Fig. 4.18. The frequency of the induced back-emf is 26.67Hz which corresponds to the rated frequency of the machine. To observe the frequency of the induced back-emf, a zoom simulation Fig. 4.19 is presented.

The controller in Simulink managed to dictate the rotor speed of the machine modeled in Maxwell to follow the reference speed as seen in Fig. 4.20 at the beginning of the simulation. When simulation reaches steady state, a load torque of -2kNm is applied to the machine model at 0.6s. The rotor speed tries to increase but the controller reacts to bring it back to reference speed as observed in Fig. 4.20. When the simulation reaches steady state again, a line to line fault is activated in the system at simulation time 1.5s. At this point, the controller losses controllability and the rotor speed behaves nasty as seen in Fig. 4.20.

Moreover, the controller manages to control the behavior of the currents which further controls the electrodynamic torque of the machine. At the very beginning part of the simulation, high currents is produced to overcome the inertia of the machine as seen in Fig. 4.21. This high initial currents results to high initial electrodynamic torque of the machine as seen in Fig. 4.23. When the machine starts to rotate, the currents and electrodynamic torque decay to zero since the machine runs at no load. However, at 0.6s, a load torque of -2kNm is applied to the machine. The controller reacts to this load torque and controls the currents drawn and there-



fore controlling electrodynamic torque of the machine as observed in Fig. 4.22 and Fig. 4.23 respectively.

When the simulation attains its steady state condition, a line to line fault is activated in the system at 1.5s. When a fault is activated, the controller losses its controllability to currents and therefore there is no controllability of the electrodynamic torque of the machine. This results the simulations from 1.5s to the end behave unpleasant as seen in Fig. 4.21 and Fig. 4.23 for currents and torque respectively.

### 5.1.5 Comparison of simulation results

The waveforms generated in Simulink alone are smooth and good. However, these do not represent the real life behavior of machines especially when considering complex machines. Simulink models of machine do not fully represent and analyze all parameters within a machine. The parameters input in Simulink S-function to represent the PMSM are armature resistance, inductance, moment of inertia of the machine, excitation magnetic flux and number of poles of the machine. However, these are not the only parameters in real machine designs. Parameters such as air gap length, size of the machine, magnetic properties, type and number of slots with related parameters, arrangement of the winding with related parameters, windage and friction losses and many other parameters are real factors to be considered in real machine designs [16].

These real parameters which can not be fully represented in Simulink simulation make a difference of the controller design for first-order harmonic models within dynamic simulation compared to controller design as a result of co-simulation.

In Simplorer, a PMSM is defined by picking a generic machine and input the design parameters. Now, in Simplorer the parameters which are input to the generic machine model are not different from the parameters input to Simulink machine model. However, due to data exchange between Simulink and Simplorer during simulation, this results to a slight changes of the controller parameters in order to produce better control signal to the machine. Control parameters such as proportional gains, integral gains, active damping for Simplorer-Simulink simulations are slightly different from Simulink simulations alone.

A big difference comes for Maxwell-Simplorer-Simulink co-simulation. A FEM model represents nearly a real life situation of the machine. More information of the machine are defined and analyzed in the FEM model. This leads to a challenging task in tuning the controller so as to control the machine in the desired way. Estimation of the machine parameters such as armature resistance, inductance, magnetization flux and others which are required as inputs to the controller to produce control signal becomes very difficult. However, using Ziegler method [17] of tuning controllers

is a better starting point for tuning the controller.

In all of the three simulations which are Simulink, Simplorer-Simulink and Maxwell-Simulink-Simplorer, the controller manages to control the torque of the machine accordingly as shown in the simulation chapter. The oscillation in the simulation is due to a too large simulation time step.

## 5.2 Conclusion

The main goal of this project which was to co-simulate a permanent magnet synchronous generator (PMSG) was attained. The research dealt more in making Simulink and Maxwell to communicate together with the help of Simplorer as interface engine. The main target has been well achieved as simulations show. The simulations also indicate the behavior of co-simulation system under fault condition. This indicates that, co-simulation between Maxwell and Simulink is possible and hence advantages of co-simulation of complex machine designs can be obtained [18].

By using FEM software, the behaviour and physics of complex machine designs can be well analyzed. When the analyzed model of the machine is then coupled to control system, it provides better information to the controller to generate reasonable control signals. This suggests that, in order to develop control strategies for complex machines, there is a need of using different designing tools. These tools are then coupled and communicated together to get a good understanding and behavior of machine designs.

The ability of integrating designs developed with different designing tools, real life situations can be achieved. Co-simulation has been approved to be appropriate and deliver viable results [2]. Again co-simulation can be a valuable solution combining models from different suppliers delivered using different modeling languages in a combined simulation environment [2].

Simplorer has played a big role in this project. It has been used as a coupling interface engine, allowing a direct co-simulation with external simulation packages. In this co-simulation, Simplorer has managed to interface Simulink, a tool used for control and Maxwell, a tool used to model and analyze machines. Both simulators are running in a call function mode and exchange data during each simulation time step [2].

There have been different approaches to model machines. Among these approaches, analytical methods have been given priority. The analytical methods are fast and also give good approximation of machine behavior [8]. However for good information representation, finite element method has been the most accurate way. The machine in this project has been modeled in Maxwell 2D. However, 3D representation is more

accurate but with the drawback of much longer simulation time.

Besides many advantages of co-simulation, the main drawback is long simulation time. In order to get precious simulations, it is required the minimum simulation time step to be as low as possible. However, the lower the minimum simulation time step gets, the longer time the simulation will take. For example for 0.1ms minimum time step and simulating for 1s time, the simulation can take up to 10hours plus taking the most memory space of the hard disk of the computer. Addition reason to long time simulation is the mesh inside the Maxwell model. The denser the mesh becomes, the higher is the accuracy of the results but the longer the simulation time [8].

### 5.3 Recommendation

Long simulation time was a huge challenge for the project. For instance, simulation for 1s could take up to 10hrs. This was a big problem especially when considering the transient behaviour of big machines with huge moment of inertia which are normally used in wind power applications.

Another thing related to simulation time, was the minimum time step for simulations. As the minimum time step of simulation was increased, the duration for simulation could decrease. However, with increase of minimum simulation time step, the simulation results were highly affected. With the lowest possible minimum simulation time step, reasonable and smooth curves could be obtained at a cost of long simulation time.

Other factors which seem to affect the co-simulation include the zero component in the quantities which make them not displaced 120 degree from one phase to another. Harmonic content in currents and voltages in Maxwell-Simplorer-Simulink co-simulation can be due to design of the winding inside the machine. Magnetization characteristics of the permanent magnet used in the machine should be well analyzed. Magnetization characteristics of the permanent magnet can also affect the behavior of the machine. There should be also losses in the magnetic core of the machine. For reduction of losses in magnetic core of generator, the level of flux density must be chosen correctly [19].

The online support for Simplorer are really good for reference. They give satisfactory explanations. On top of that they usually give an example for the topic concerned. Most components have their mathematical descriptions and therefore, it is simple to follow and make a correct model of the intended component. On the other hand, Maxwell documentation though helped but it was not easy to follow. There are not enough documentation on different topics. Furthermore, no examples to show how to go through. This makes a user spend a lot of time to find out how to use different parameters in Maxwell.

## 5.4 Future work

It has been observed that the output performance of the co-simulation can be affected with machine parameters in the Maxwell model. When there are variations in air gap length, strength of magnetizing flux, type and arrangement of slots, machine size, type and arrangement of winding affect the behaviour of the controller. Therefore, in order to generate good control signal to the machine, more studies should be done on the FEM model so that it provides reasonable feedback signals to the controller and hence the controller produces reasonable control signals back to the machine.

The load type connected to the machine also affects the behaviour of the simulation. Different load types in Simpler have different behaviour. So there should be more study on which type of load to be connected to the FEM model to get reasonable simulations instead of using blocks to model the mechanical dynamics.

In reality a converter should be placed between the control system model and the machine model. This suggests that there should be studies also which will place the converter in the system and see how the co-simulation will behave.

# References

- [1] O. Haedrich, *Electric Circuit and Control System Simulation by Linking Simplorer and Matlab/Simulink - Analysis of Interactions of Subsystems of Modern Electric Drives*, 0-7803-6561-5 ed., July 2000.
- [2] D. E. Knorr and D. R. Juchem, *A complete co-simulation-based design environment for electric and hybrid-electric vehicles, fuel-cell systems, and drive trains*, sae technical paper 2003-01-1140, 2003, doi:10.4271/2003-01-1140. ed., 3rd March 2003.
- [3] C. N. Bhende, S. Mishra, and S. G. Malla, *IEEE Permanent Magnet Synchronous Generator-Based Standalone Wind Energy Supply System*, vol. 2, no. 4 ed., October 2011.
- [4] K.-J. Ko, S.-M. Jang, J.-H. Park, H.-W. Cho, and D.-J. You, *IEEE Electromagnetic Performance Analysis of Wind Power Generator With Outer Permanent Magnet Rotor Based on Turbine Characteristics Variation Over Nominal Wind Speed*, vol. 47, no. 10 ed., October 2011.
- [5] F. Wang, Q. Hou, J. Bo, and J. Pan, *IEEE Study on Control System of Low Speed PM Generator Direct Driven by Wind Turbine*, 10.1109/icems.2005.202697, 1009-1012 vol.2 ed., IEEE Power Engineering Society 2005.
- [6] L. Harnefors, *Control of Variable-Speed Drives*. Department of electronics, Mälardalen University, Västerås, Sweden: Applied signal processing and control, 2002.
- [7] “Power electronic devices and applications enm070.” Lecture Slides Week 4, Q4 2012.
- [8] M. Salman, *Analysis, design and control aspects of linear machines using co-simulation*, xr-ee-e2c 2012:001 ed., 2012.
- [9] C. Ogbuka, O. Okoro, and M. Agu, *Solving Electrical Circuits Transient Problems with MATLAB and SIMPLORER*, volume 9. number 1. ed., May-June 2008.
- [10] S. Lorand and D. J. Barna, *Coupled Simulink-Simplorer Model of a Modular Hybrid Linear Stepper Motor*, issn: 1401-5757, uptec f11 028 ed.
- [11] A. Corporation, *Getting Started with Simplorer*, simplorer11 ed., November 2012.
- [12] A. Corporation, *RMxpert Manual*, chapter 1: introduction ed.

- [13] A. Corporation, *RMxprt Manual*, chapter 15: adjust-speed permanent-magnet synchronous machines ed.
- [14] Ansys, *Simplorer Co-Simulation with Maxwell*, simplorer11 ed.
- [15] S. Engstrom, *The NewGen direct drive generator for large wind turbines*, newgen generator ab ed., March 2011.
- [16] J. Pyrhönen, T. Jokinen, and V. Hrabovcová, *Design Process and Properties of Rotating Electric Machines*.
- [17] V. Tootchinda, *Digital PID Controllers*, June 2011.
- [18] T.-M. Wolter, J. Kitte, and S. Kulawik, *Benefits of Co-Simulation in the Development Process of Hybrid Vehicles*. Carnotstrasse1, 10587 BERLIN (GERMANY): International Conference on Advances in Hybrid Powertrains, November, 2008.
- [19] A. Kilik and O. Kudrjavnsev, *IEEE Study and Verification of a Slow Speed PM Generator with Outer Rotor for Small Scale Wind Turbines*, 978-1-4673-1978-2 ed., IEEE Power Engineering Society 2012.

# Appendix A

## ASPMSM Design Data

<b>GENERAL DATA</b>	
Rated Output Power (kW):	120
Rated Voltage (V):	220
Number of Poles:	32
Frequency (Hz):	26,6667
Frictional Loss (W):	0
Windage Loss (W):	0
Rotor Position:	Outer
Type of Circuit:	Y3
Type of Source:	Sine
Domain:	Time
Operating Temperature (C):	75
<b>STATOR DATA</b>	
Number of Stator Slots:	168
Outer Diameter of Stator (mm):	1600
Inner Diameter of Stator (mm):	1300
Type of Stator Slot:	4
Stator Slot	
hs0 (mm):	2,5
hs1 (mm):	0
hs2 (mm):	76
bs0 (mm):	4
bs1 (mm):	11,3
bs2 (mm):	11,3
rs (mm):	0

Figure A.1: ASPMSM Design Data page 1

Top Tooth Width (mm):	18,5266
Bottom Tooth Width (mm):	15,6843
Skew Width (Number of Slots):	0
Length of Stator Core (mm):	140
Stacking Factor of Stator Core:	0,95
Type of Steel:	M19_24G
Designed Wedge Thickness (mm):	0
Slot Insulation Thickness (mm):	0,3
Layer Insulation Thickness (mm):	0
End Length Adjustment (mm):	0
Number of Parallel Branches:	4
Number of Conductors per Slot:	17
Type of Coils:	11
Average Coil Pitch:	4,71429
Number of Wires per Conductor:	4
Wire Diameter (mm):	2,906
Wire Wrap Thickness (mm):	0
Slot Area (mm <sup>2</sup> ):	868,8
Net Slot Area (mm <sup>2</sup> ):	803,03
Limited Slot Fill Factor (%):	75
Stator Slot Fill Factor (%):	71,5103
Coil Half-Turn Length (mm):	357,067
Wire Resistivity (ohm.mm <sup>2</sup> /m):	0,0217

Figure A.2: ASPMSM Design Data page 2



<b>ROTOR DATA</b>	
Minimum Air Gap (mm):	25
Outer Diameter (mm):	1798
Length of Rotor (mm):	140
Stacking Factor of Iron Core:	0,95
Type of Steel:	M19_24G
Polar Arc Radius (mm):	825
Mechanical Pole Embrace:	0,7
Electrical Pole Embrace:	0,664286
Max. Thickness of Magnet (mm):	22
Width of Magnet (mm):	113,303
Type of Magnet:	XG196/96
Type of Rotor:	1
Magnetic Shaft:	No
<b>PERMANENT MAGNET DATA</b>	
Residual Flux Density (Tesla):	1,08671
Coercive Force (kA/m):	864,775
Maximum Energy Density (kJ/m <sup>3</sup> ):	234,939
Relative Recoil Permeability:	1,00003
Demagnetized Flux Density (Tesla):	0
Recoil Residual Flux Density (Tesla):	1,08671
Recoil Coercive Force (kA/m):	864,775

Figure A.3: ASPMSM Design Data page 3

<b>MATERIAL CONSUMPTION</b>	
Armature Wire Density (kg/m <sup>3</sup> ):	8900
Permanent Magnet Density (kg/m <sup>3</sup> ):	7800
Armature Core Steel Density (kg/m <sup>3</sup> ):	7650
Rotor Core Steel Density (kg/m <sup>3</sup> ):	7650
Armature Copper Weight (kg):	240,79
Permanent Magnet Weight (kg):	88,3343
Armature Core Steel Weight (kg):	546,715
Rotor Core Steel Weight (kg):	290,209
Total Net Weight (kg):	1166,05
Armature Core Steel Consumption (kg):	2053,38
Rotor Core Steel Consumption (kg):	1246,82
<b>STEADY STATE PARAMETERS</b>	
Stator Winding Factor:	0,931856
D-Axis Reactive Reactance X <sub>ad</sub> (ohm):	0,0664922
Q-Axis Reactive Reactance X <sub>aq</sub> (ohm):	0,0664922
D-Axis Reactance X <sub>1</sub> +X <sub>ad</sub> (ohm):	0,217676
Q-Axis Reactance X <sub>1</sub> +X <sub>aq</sub> (ohm):	0,217676
Armature Leakage Reactance X <sub>1</sub> (ohm):	0,151184
Zero-Sequence Reactance X <sub>0</sub> (ohm):	0,151184
Armature Phase Resistance R <sub>1</sub> (ohm):	0,0173774
Armature Phase Resistance at 20C (ohm):	0,0142943

Figure A.4: ASPMSM Design Data page 4

<b>NO-LOAD MAGNETIC DATA</b>	
Stator-Teeth Flux Density (Tesla):	1,16136
Stator-Yoke Flux Density (Tesla):	0,462074
Rotor-Yoke Flux Density (Tesla):	0,635352
Air-Gap Flux Density (Tesla):	0,443272
Magnet Flux Density (Tesla):	0,583814
Stator-Teeth By-Pass Factor:	0,000233823
Stator-Yoke By-Pass Factor:	7,81E-06
Rotor-Yoke By-Pass Factor:	8,08E-06
Stator-Teeth Ampere Turns (A.T):	21,9496
Stator-Yoke Ampere Turns (A.T):	2,85526
Rotor-Yoke Ampere Turns (A.T):	5,07138
Air-Gap Ampere Turns (A.T):	8771,26
Magnet Ampere Turns (A.T):	-8804,19
Leakage-Flux Factor:	1
Correction Factor for Magnetic Circuit Length of Stator Yoke:	0,778571
Correction Factor for Magnetic Circuit Length of Rotor Yoke:	0,763989
No-Load Line Current (A):	61,908
No-Load Input Power (W):	454,778
Cogging Torque (N.m):	3,27819

Figure A.5: ASPMSM Design Data page 5

<b>FULL-LOAD DATA</b>	
Maximum Line Induced Voltage (V):	278,899
Root-Mean-Square Line Current (A):	364,836
Root-Mean-Square Phase Current (A):	364,836
Armature Thermal Load (A <sup>2</sup> /mm <sup>3</sup> ):	178,165
Specific Electric Loading (A/mm):	51,8234
Armature Current Density (A/mm <sup>2</sup> ):	3,43793
Frictional and Windage Loss (W):	0
Iron-Core Loss (W):	252,615
Armature Copper Loss (W):	6939,07
Total Loss (W):	7191,69
Output Power (W):	120037
Input Power (W):	127229
Efficiency (%):	94,3474
Synchronous Speed (rpm):	100
Rated Torque (N.m):	11462,7
Torque Angle (degree):	38,1721
Maximum Output Power (W):	182283
Torque Constant KT (Nm/A):	31,4188

Figure A.6: ASPMSM Design Data page 6

<b>WINDING ARRANGEMENT</b>	
The 3-phase, 1-layer winding can be arranged in 42 slots as below:	
AAZZBBXCCYYAAZBBXXCCYAZZBBXXCYAAZZBXXCCYY	
PhaseA average coil pitch is:	4,71429
PhaseB average coil pitch is:	4,71429
PhaseC average coil pitch is:	4,42857
Angle per slot (elec. degrees):	34,2857
Phase-A axis (elec. degrees):	102,857
First slot center (elec. degrees):	0
<b>TRANSIENT FEA INPUT DATA</b>	
For Armature Winding:	
Number of Turns:	476
Parallel Branches:	4
Terminal Resistance (ohm):	0,017377
End Leakage Inductance (H):	0,000235
2D Equivalent Value:	
Equivalent Model Depth (mm):	140
Equivalent Stator Stacking Factor:	0,95
Equivalent Rotor Stacking Factor:	0,95
Equivalent Br (Tesla):	1,08671
Equivalent Hc (kA/m):	864,775
Estimated Rotor Inertial Moment (kg m <sup>2</sup> ):	764,333

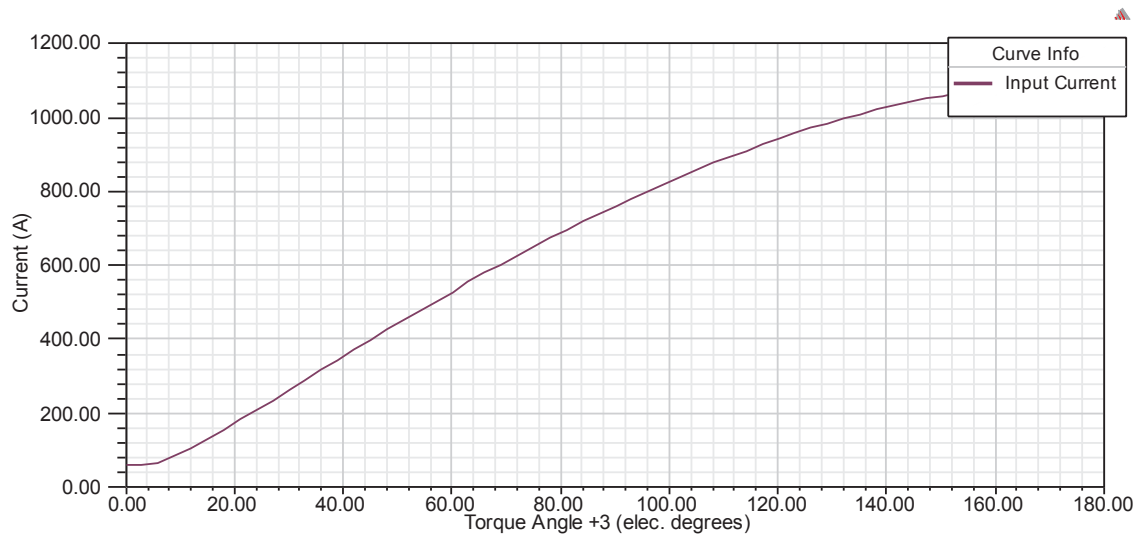
Figure A.7: ASPMSM Design Data page 7



# Appendix B

## RMxpirt Design graphs

INPUT CURRENT VS TORQUE ANGLE



EFFICIENCY VS TORQUE ANGLE

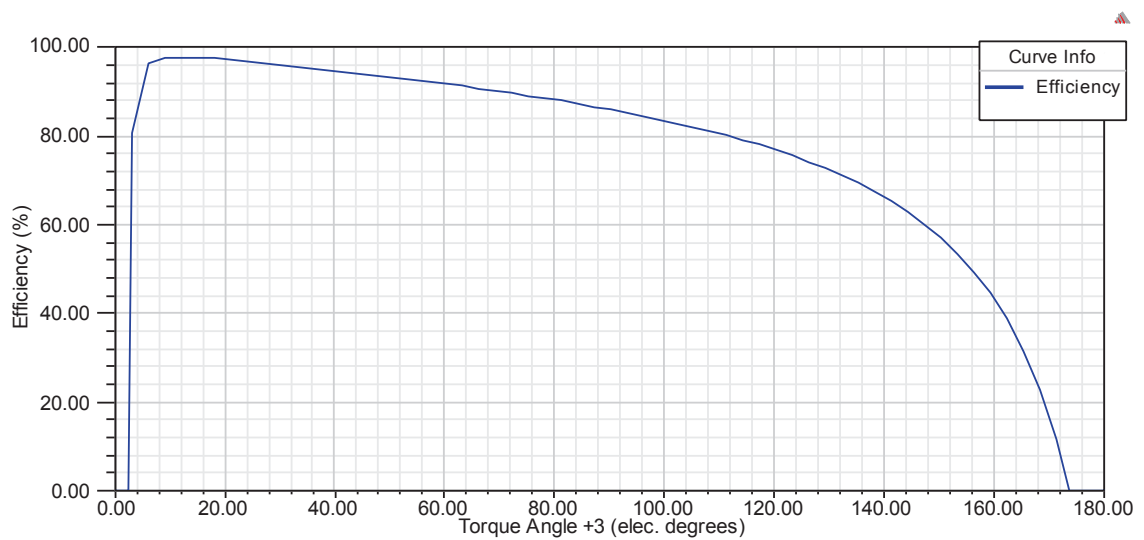
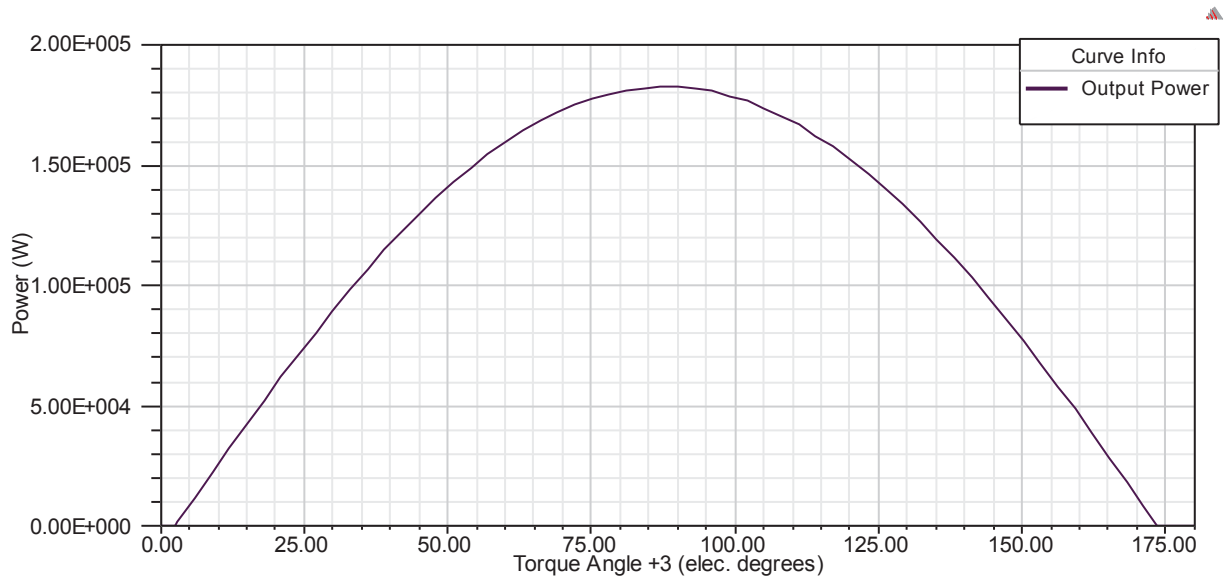


Figure B.1: RMxpirt Design graphs page 1

### OUTPUT POWER VS TORQUE ANGLE



### COGGING TORQUE IN TWO TEETH

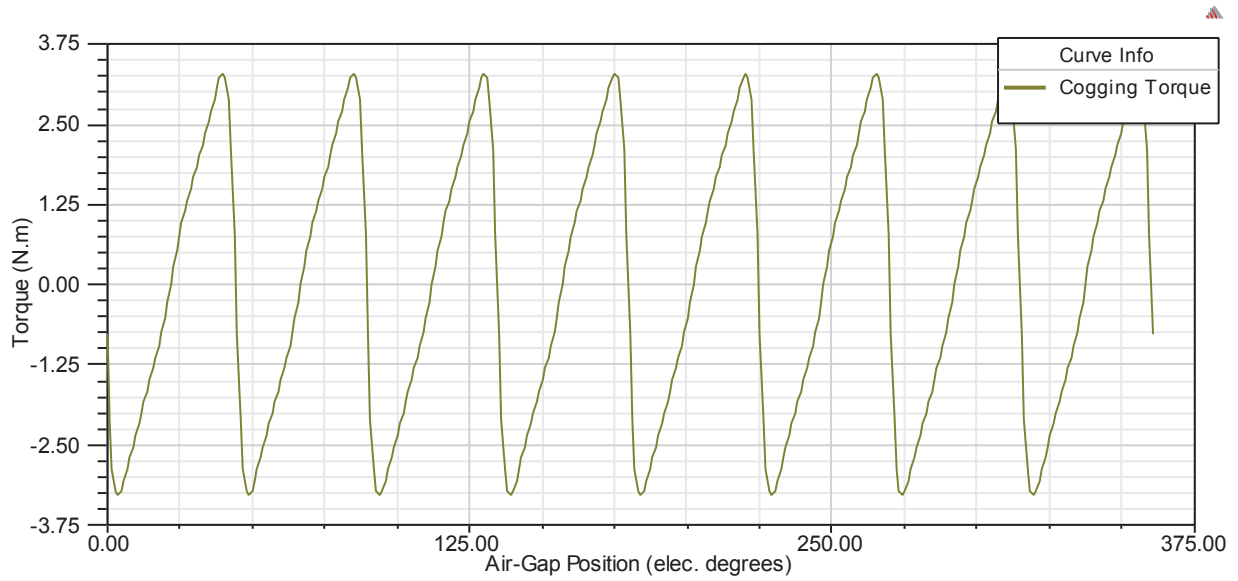
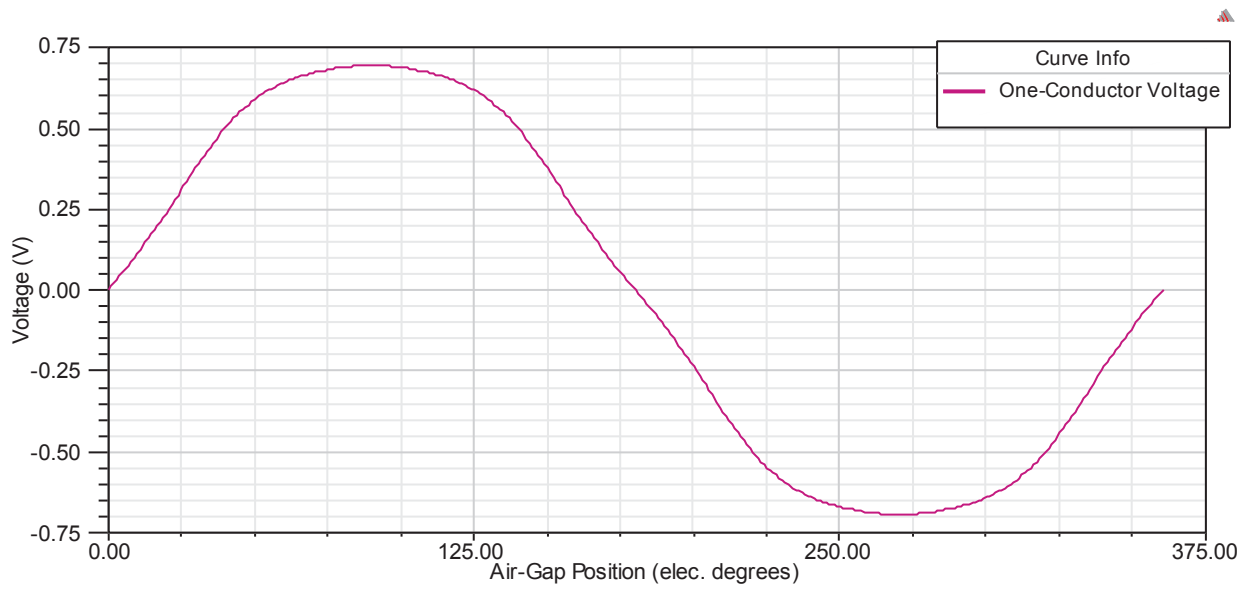


Figure B.2: RMxpert Design graphs page 2



# ONE CONDUCTOR INDUCED VOLTAGE AT RATED SPEED



# AIR-GAP FLUX DENSITY

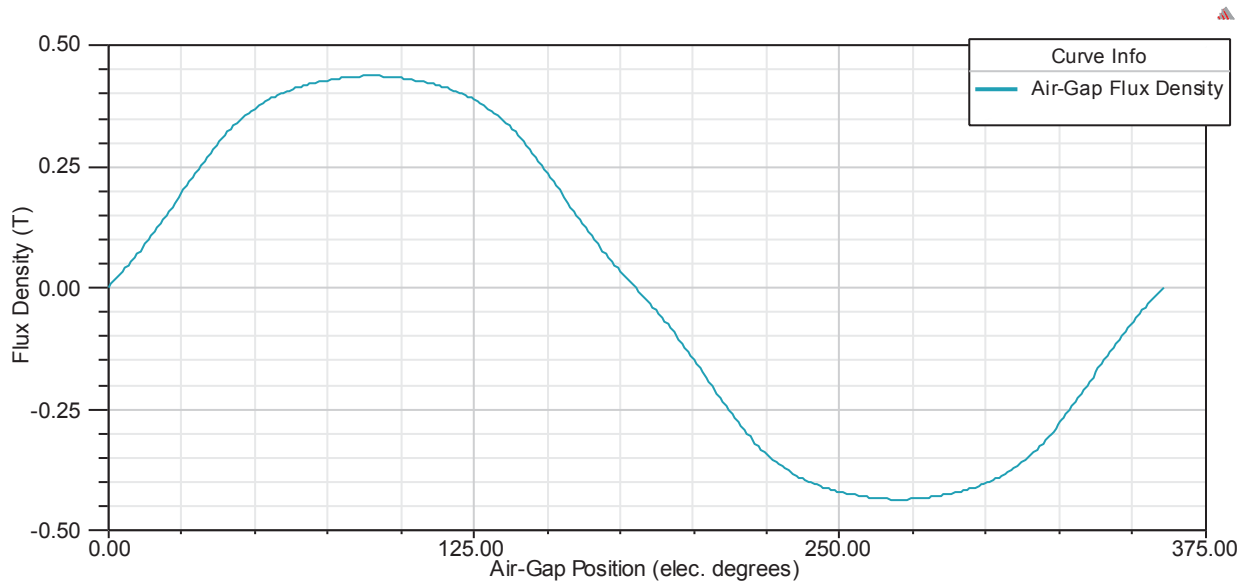
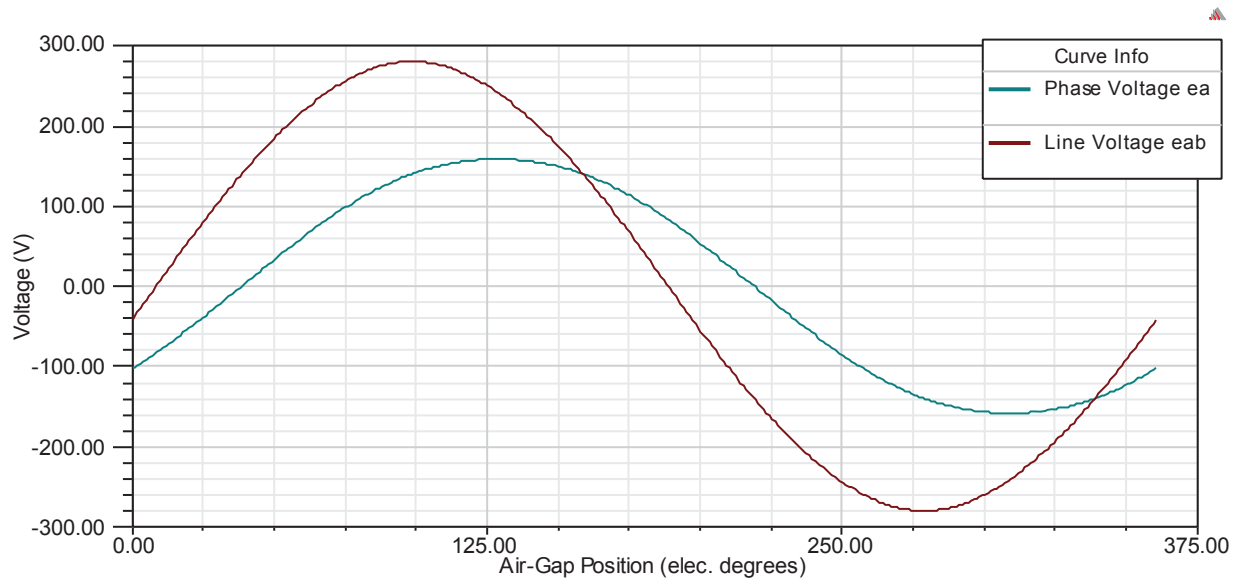


Figure B.3: RMaxprt Design graphs page 3

# INDUCED WINDING VOLTAGE AT RATED SPEED



# WINDING CURRENTS UNDER LOAD

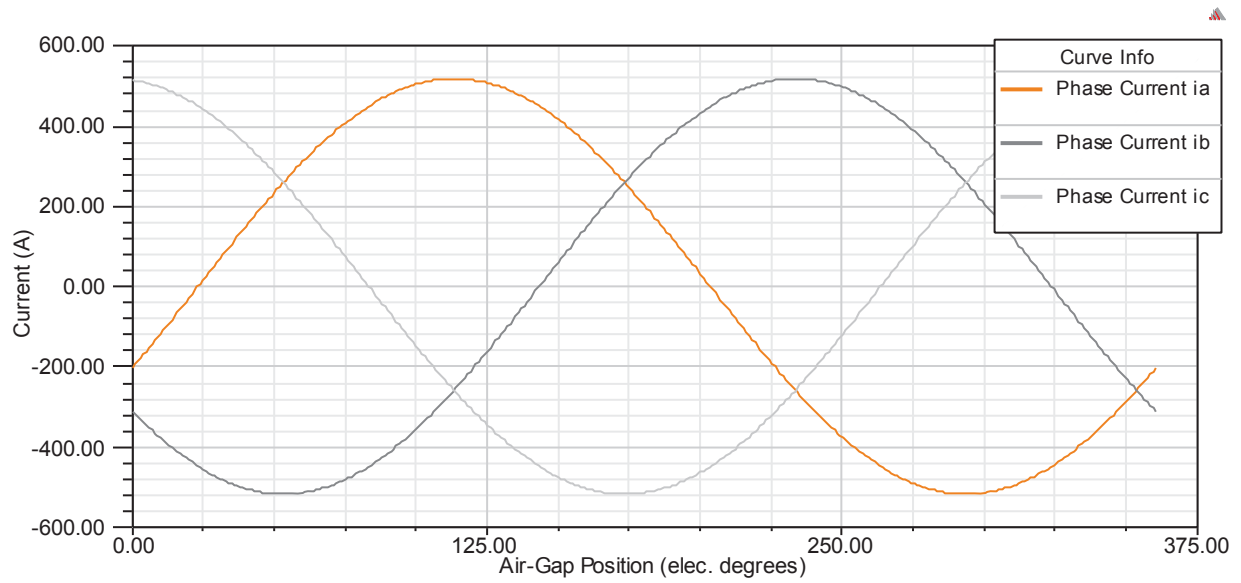


Figure B.4: RMxprt Design graphs page 4

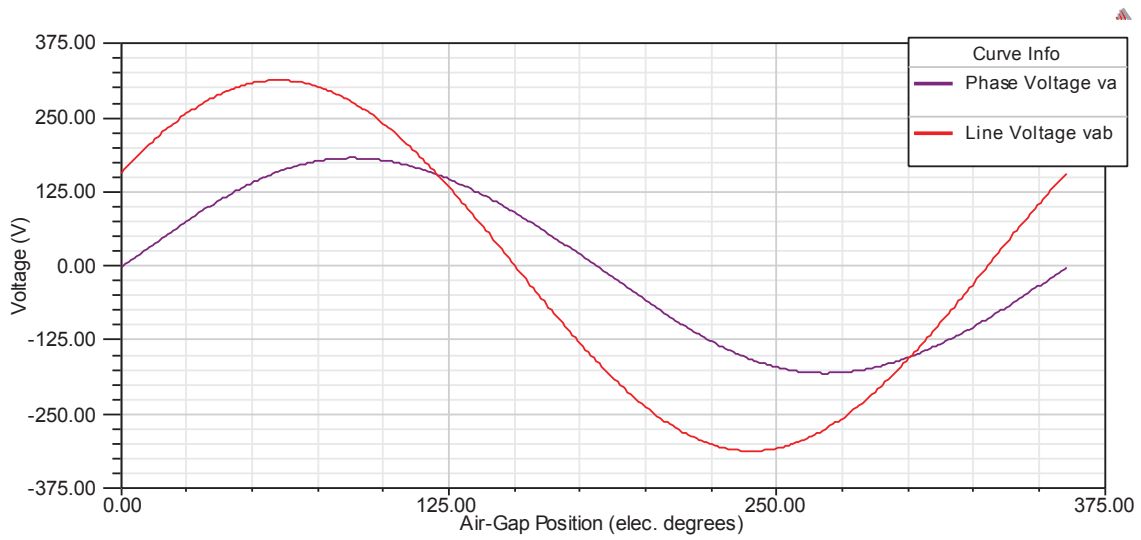


Figure B.5: RMaxprt Design graphs page 5